



Recent STAR results on strangeness production

Xianglei Zhu

Tsinghua University

11/3/2024

The 1st International Workshop on Physics at High Baryon Density (PHD2024)

CCNU, Wuhan, 2024.11.1-4

Why strangeness?

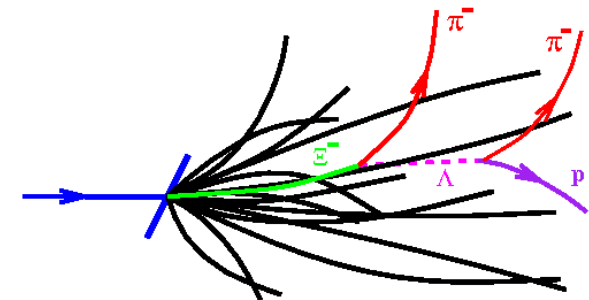
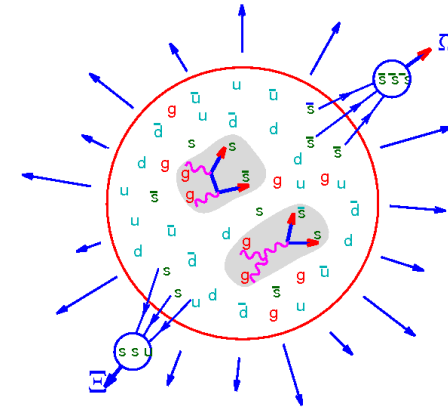
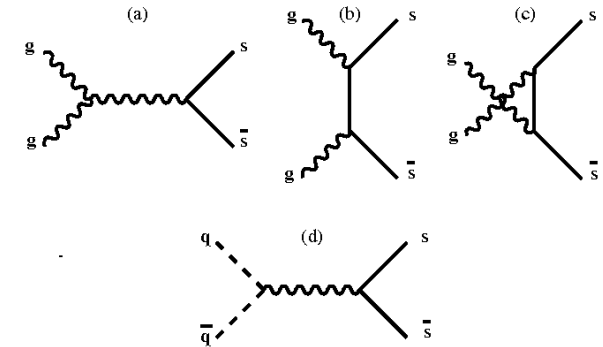
- Strange quarks
 - Not exist in colliding nuclei
 - Current mass $\sim 100 \text{ MeV} < T_c$
 - Easily pair-produced in de-confined QGP medium

→ **Strangeness enhancement !**

- Hadrons with (multiple) strange quarks
 - Small hadronic cross section
 - Sensitive to the early stage dynamics of the medium
 - Can be easily reconstructed and identified in experiment, up to high p_T !

→ **Systematic study of medium properties!**

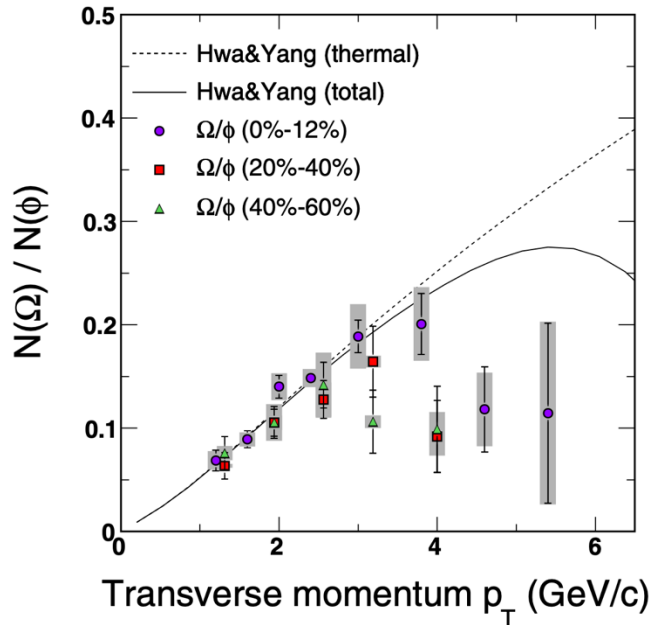
Rafelski & Müller, 1982



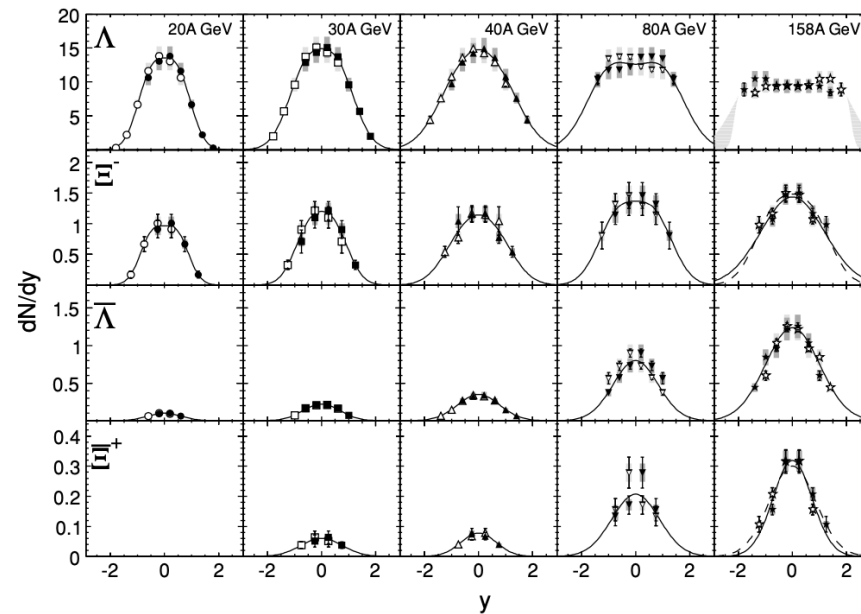
Strange hadron observables

- Nuclear modification factor of strange hadrons to evaluate the partonic energy loss in deconfined medium.
- Strange baryon-to-meson ratio can be utilized to understand hadronization mechanism.
- Rapidity density of (anti-)strange baryons may give insight on the baryon stopping mechanism.

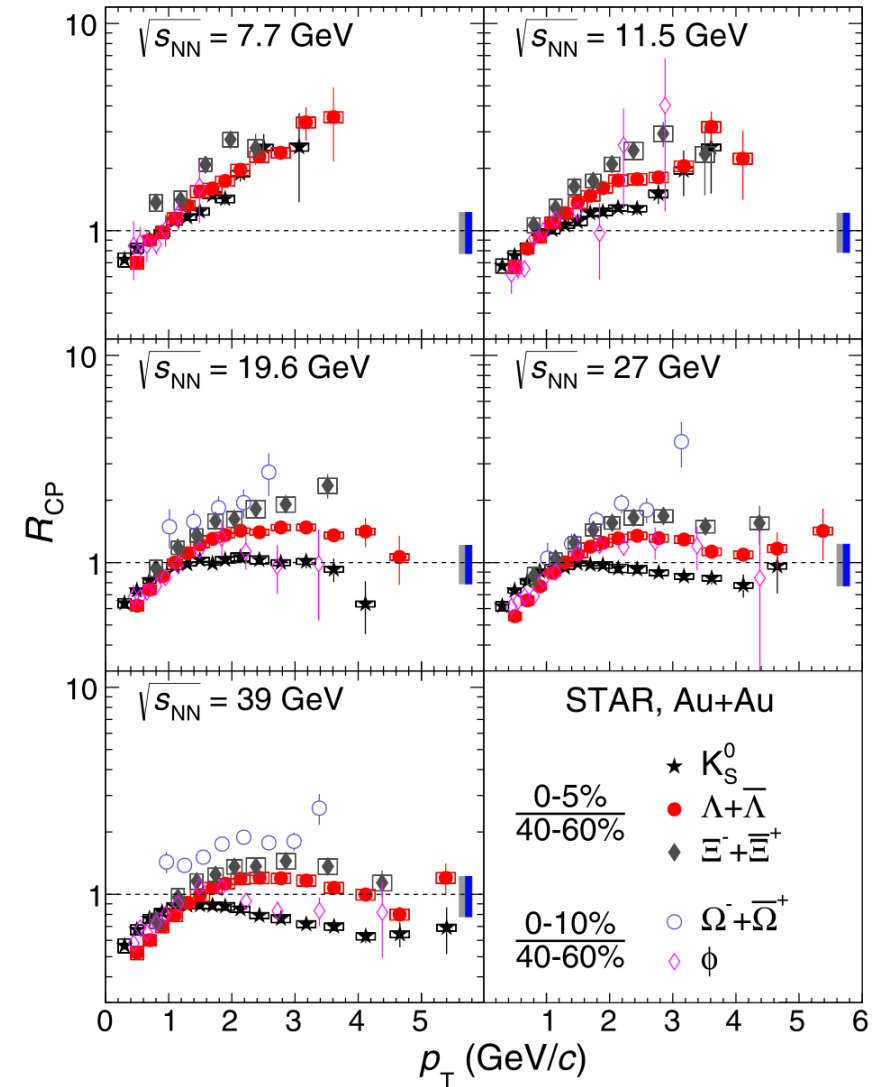
$$R_{CP} = \frac{[(dN/dp_T)/\langle N_{coll} \rangle]_{\text{central}}}{[(dN/dp_T)/\langle N_{coll} \rangle]_{\text{peripheral}}}$$



STAR, PRL 99, 112301 (2007)



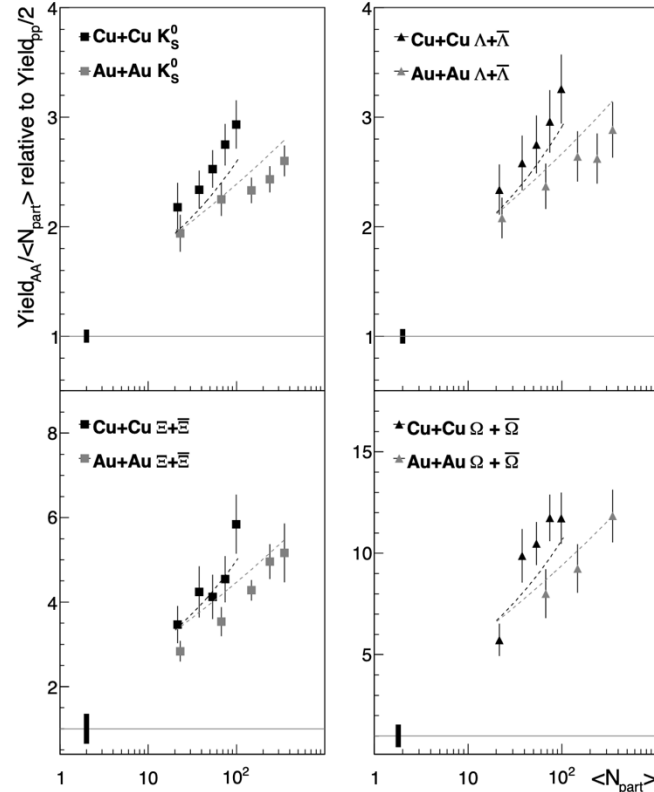
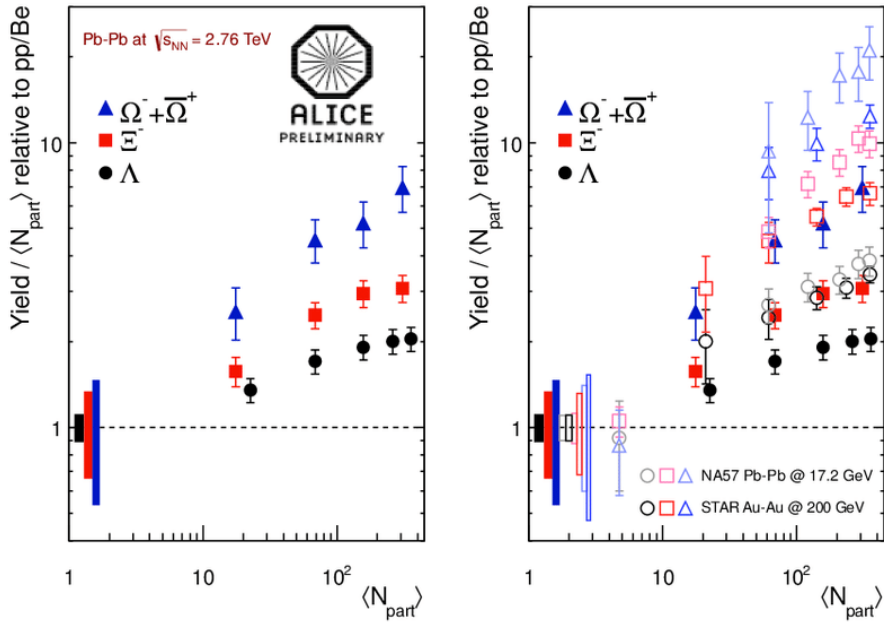
NA49, PRC 78, 034918 (2008)



STAR, PRC 102, 034909 (2020)

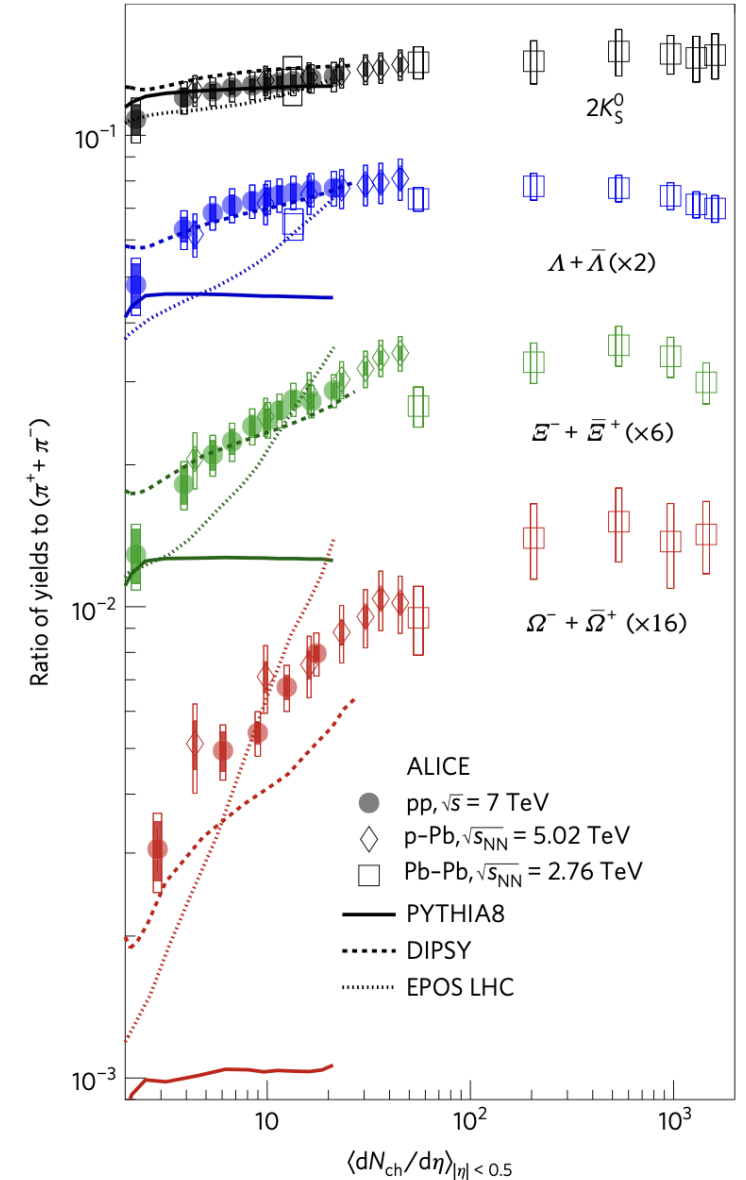
Strange hadron observables

- Strange hadron yields per N_{part} relative to pp:
 - strangeness enhancement (or canonical suppression in pp/pA)
 - system size dependence (Au+Au versus Cu+Cu)
- Strange-to-pion yield ratios:
 - strangeness enhancement in small system



STAR, Phys. Rev. Lett. **108** (2012) 72301

ALICE, Nature Physics, **13**, pages535–539 (2017)



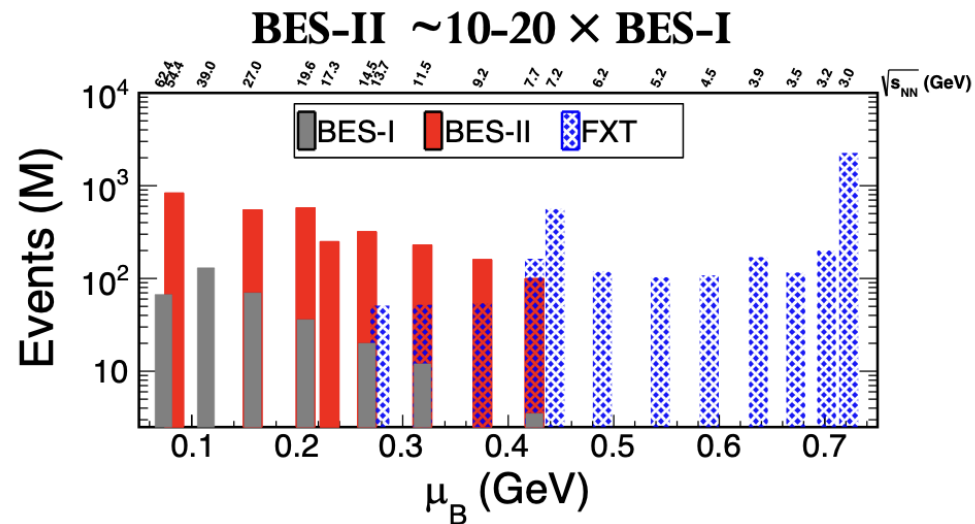
Motivation

Heavy-ion collisions at top RHIC energy:

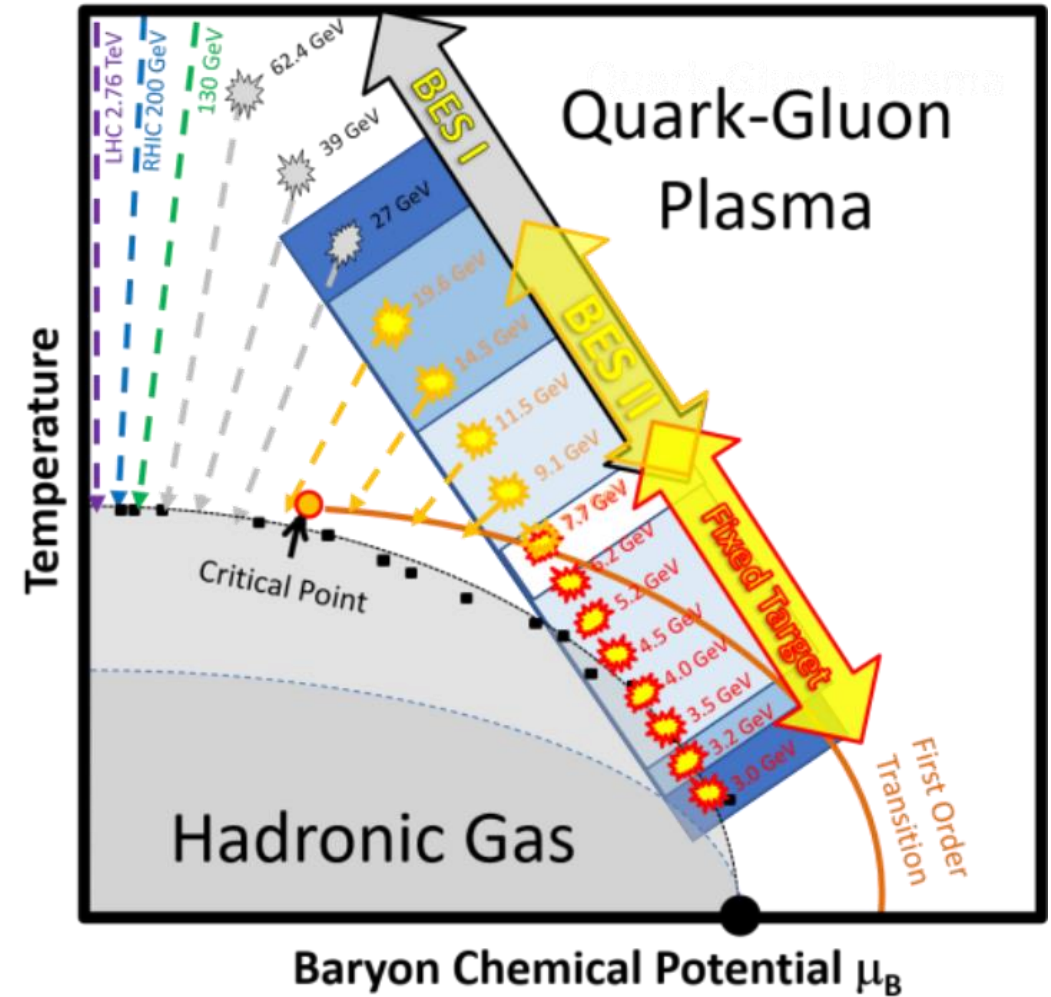
- Study QGP properties (AuAu)
- System size dependence (pp/dAu/OO/Isobar/AuAu)

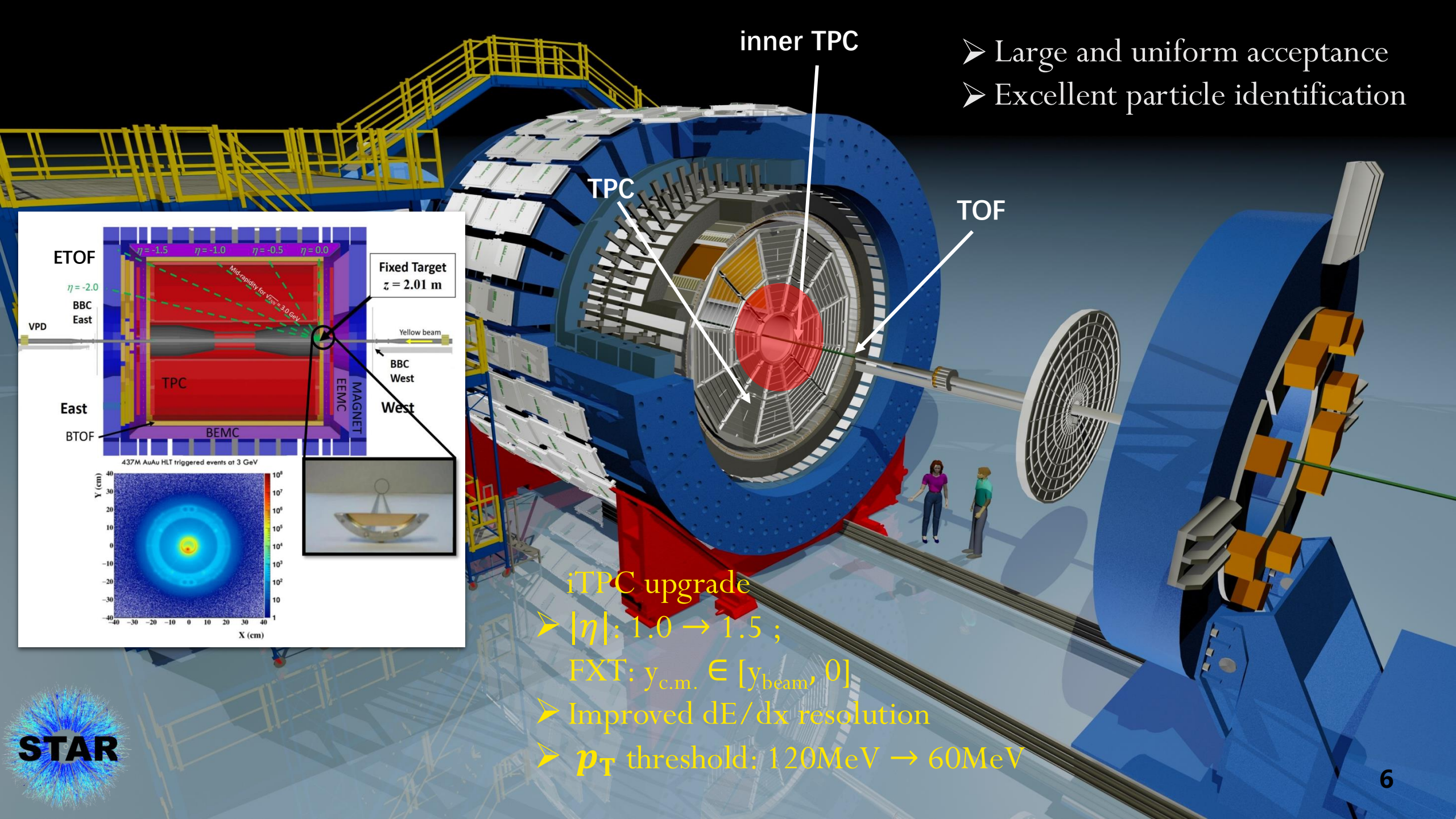
Beam Energy Scan (BES) program:

- Search for the onset of deconfinement
- Search for the first-order phase transition
- Search for the critical point

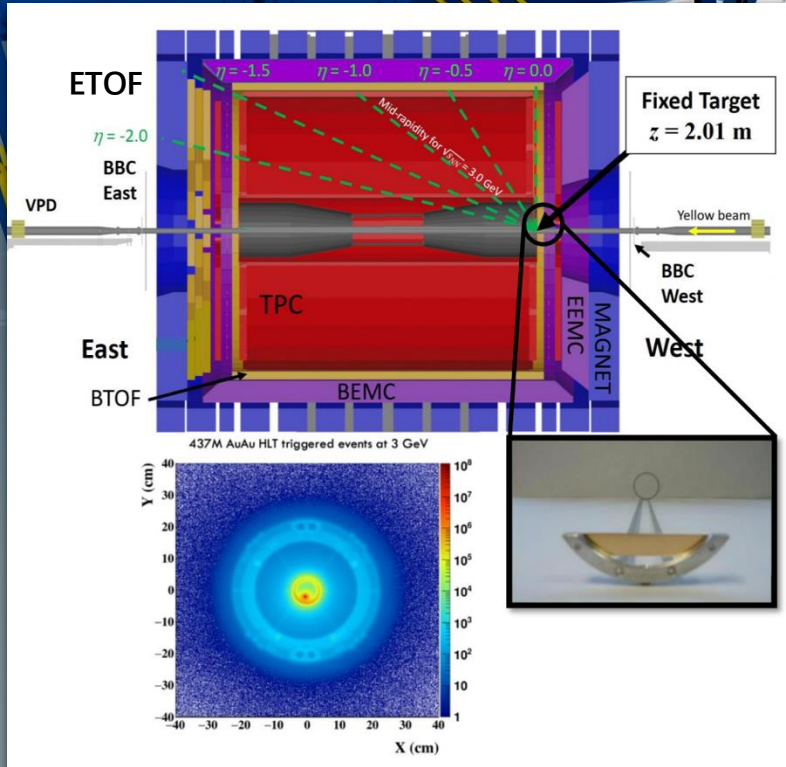


Yi Fang, Xiongxiang Xu, Weiguang Yuan, QM23/SQM24/CPS24
 Yan Huang, SQM21
 Hongcan Li, Dongsheng Li, Ishu Aggarwal, SQM24
 Yingjie Zhou, iHIC24, Iris Ponce, DNP24



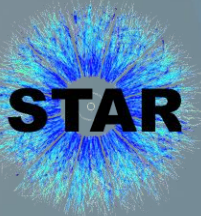


- Large and uniform acceptance
- Excellent particle identification

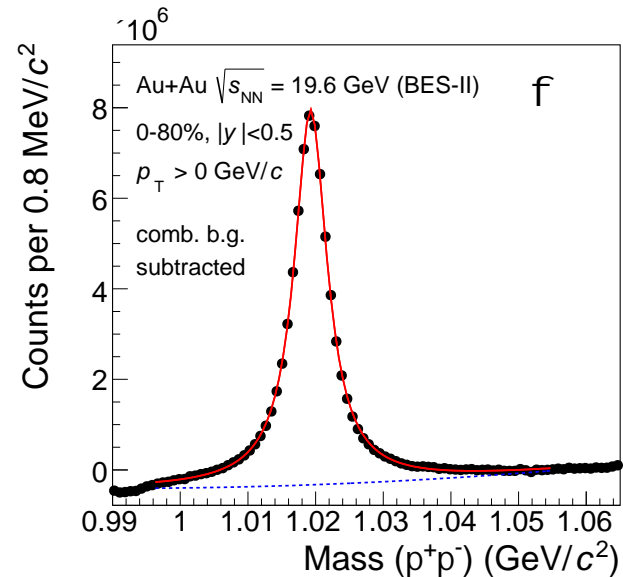
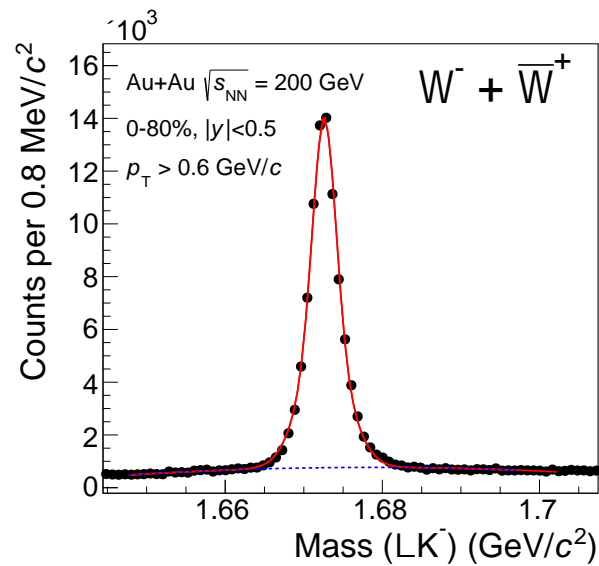
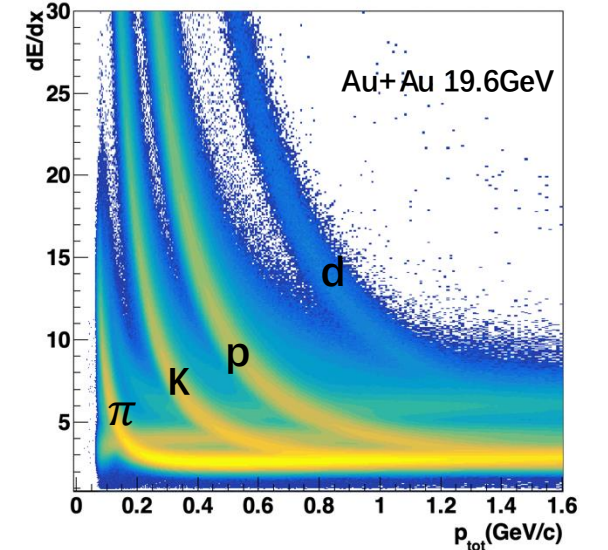
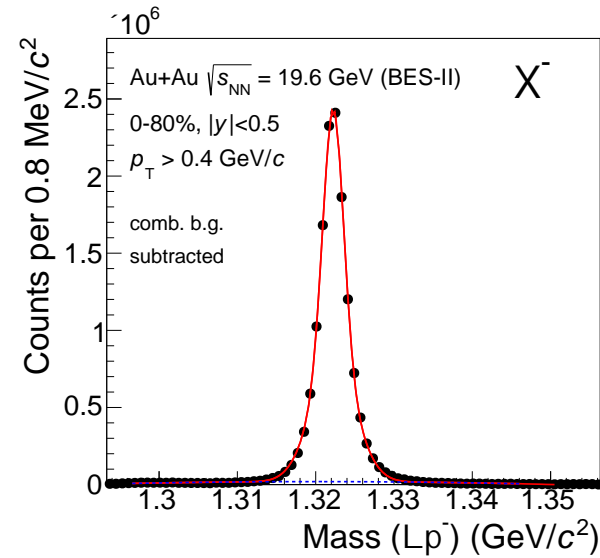
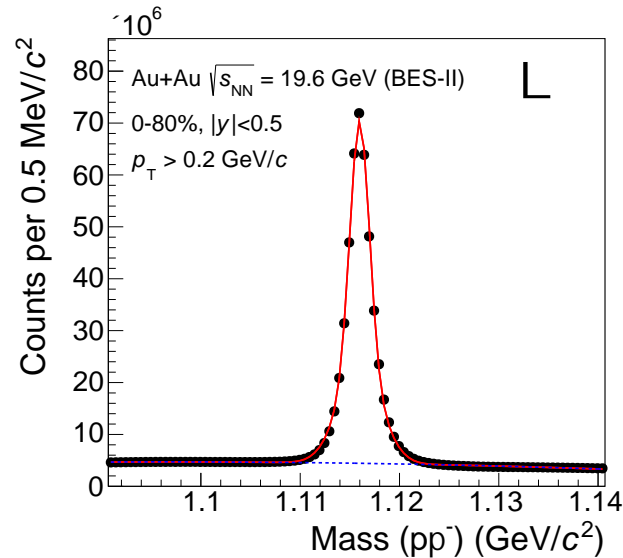
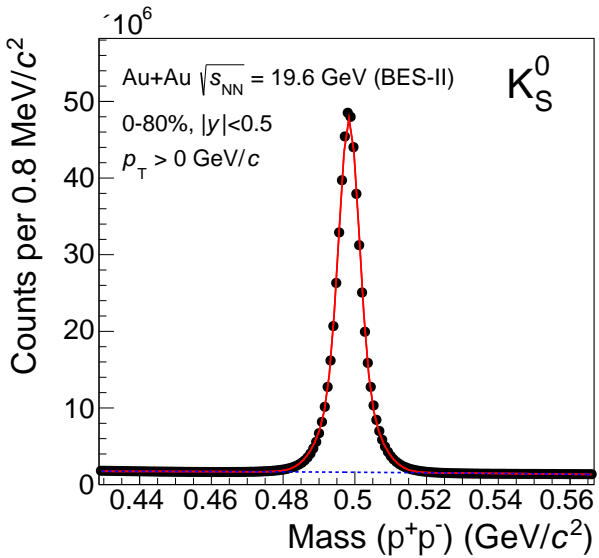


iTPC upgrade

- $|\eta|: 1.0 \rightarrow 1.5$;
- FXT: $y_{c.m.} \in [y_{beam}, 0]$
- Improved dE/dx resolution
- p_T threshold: $120\text{MeV} \rightarrow 60\text{MeV}$



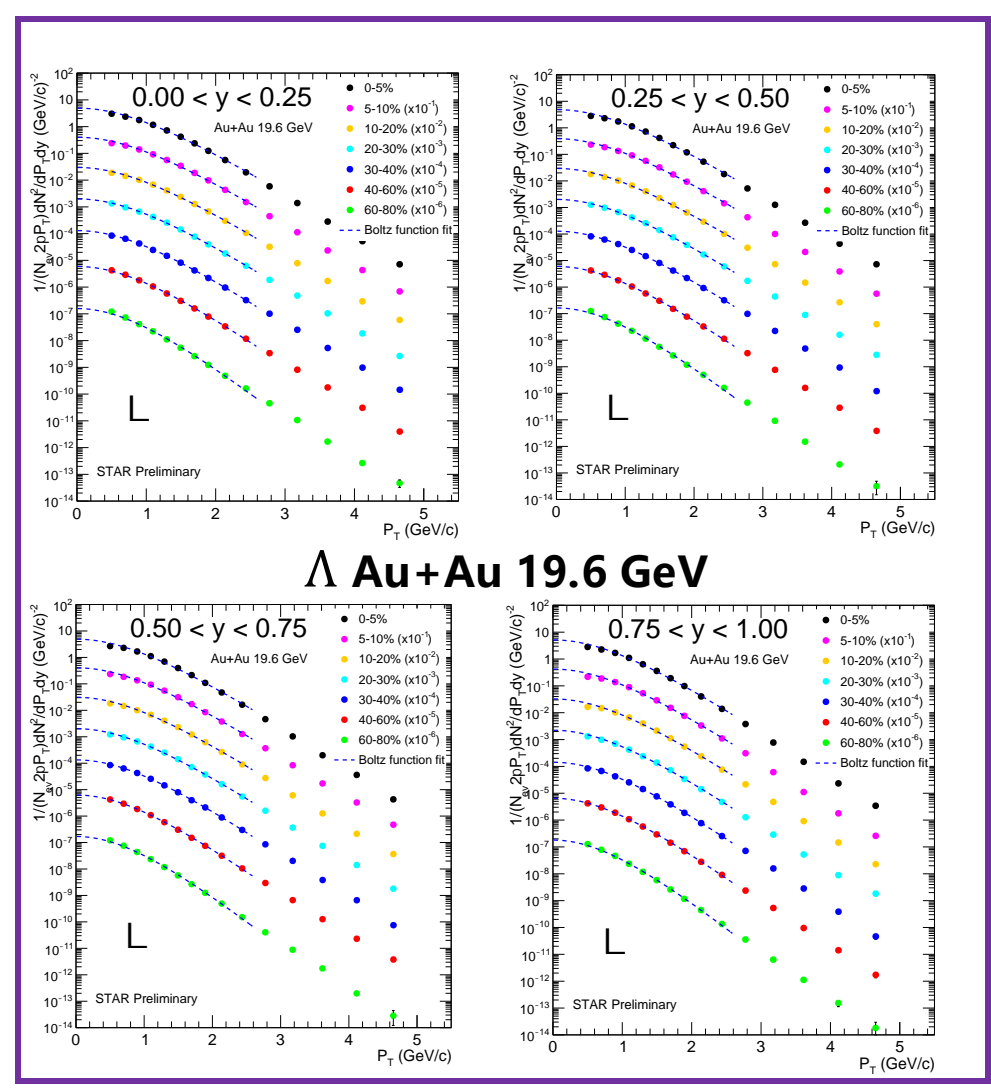
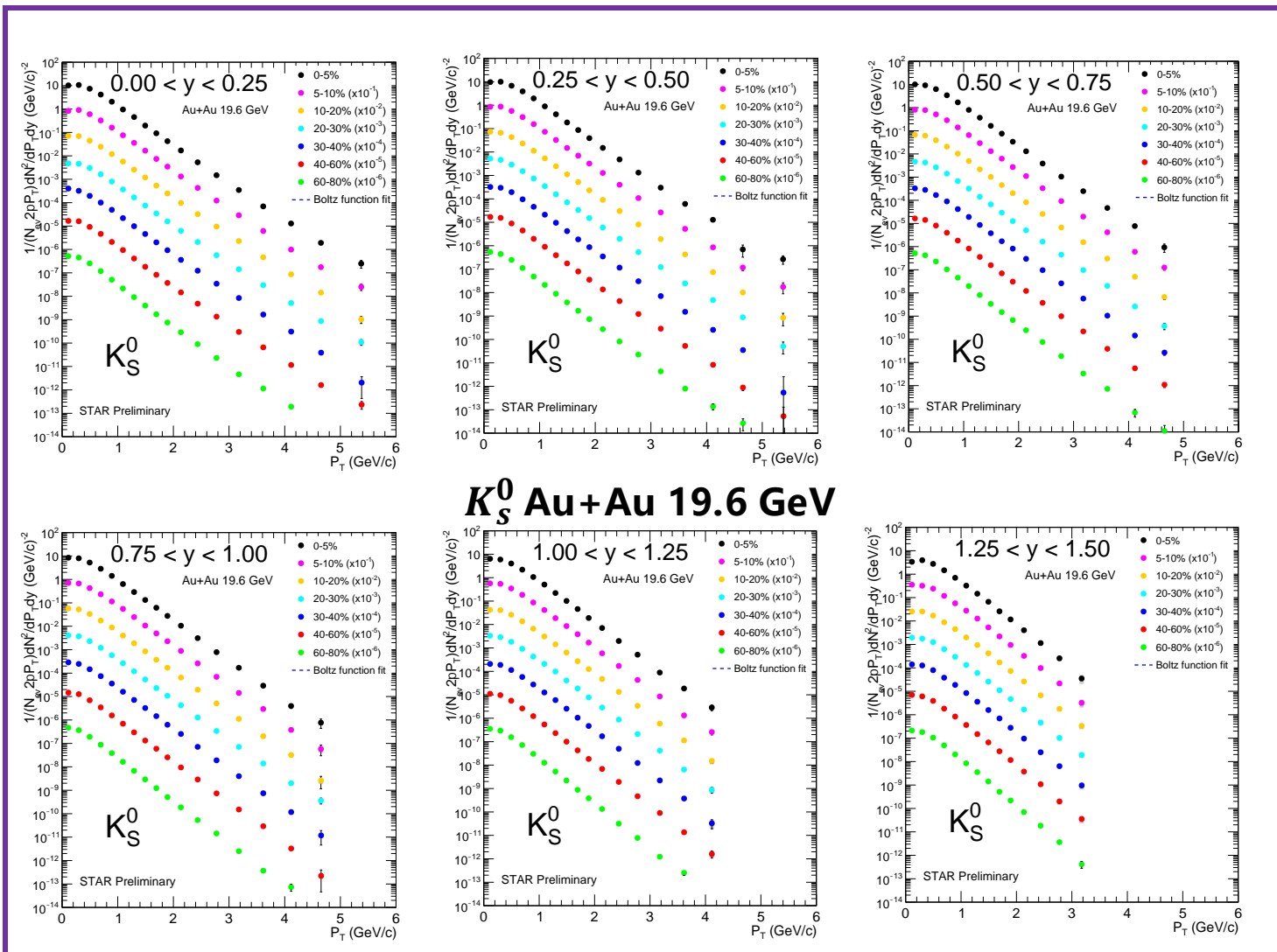
Particle identification and reconstruction



- Particle identification with dE/dx .
- π, K, p are used to reconstruct the secondary vertex of strange particles.
- TMVA optimization to improve Ω signal significance
- Large number of strange particles allow multi-differential measurements.

$$\begin{aligned}
 K_S^0 &\rightarrow \pi^+ + \pi^- (\mathcal{B} = 69.2\%) \\
 \Lambda(\bar{\Lambda}) &\rightarrow p(\bar{p}) + \pi^- (\pi^+) (\mathcal{B} = 63.9\%) \\
 \Xi^- (\bar{\Xi}^+) &\rightarrow \Lambda(\bar{\Lambda}) + \pi^- (\pi^+) (\mathcal{B} = 99.9\%) \\
 \Omega^- (\bar{\Omega}^+) &\rightarrow \Lambda(\bar{\Lambda}) + K^- (K^+) (\mathcal{B} = 67.8\%) \\
 \phi &\rightarrow K^+ + K^- (\mathcal{B} = 49.1\%)
 \end{aligned}$$

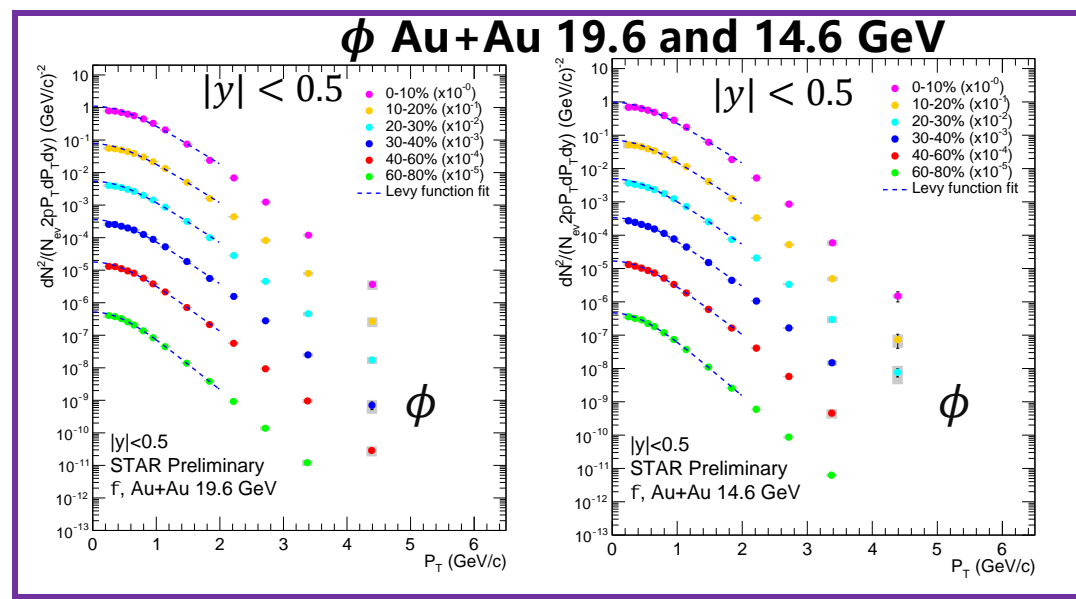
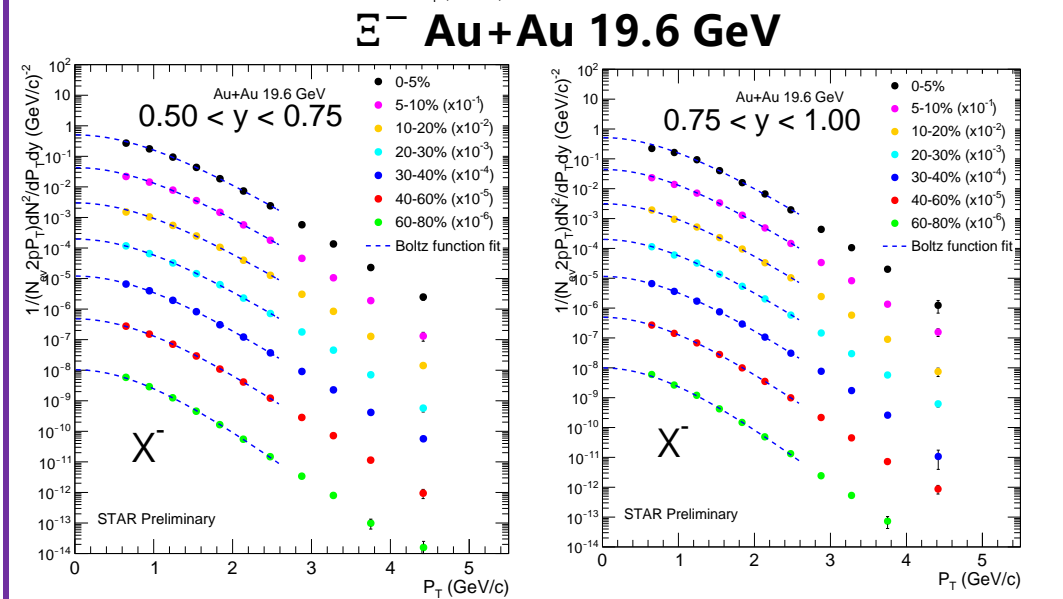
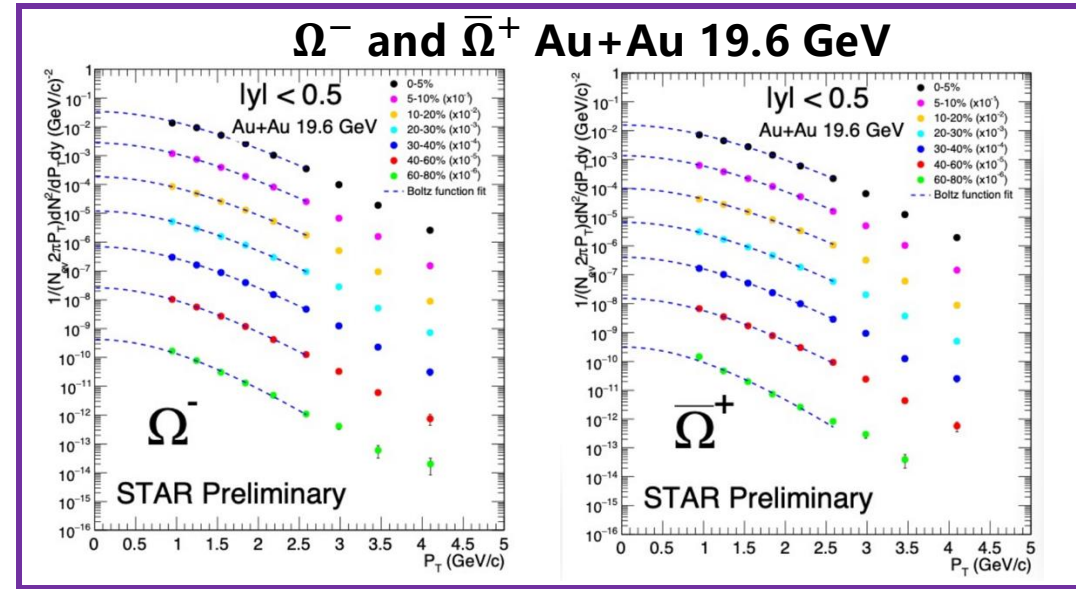
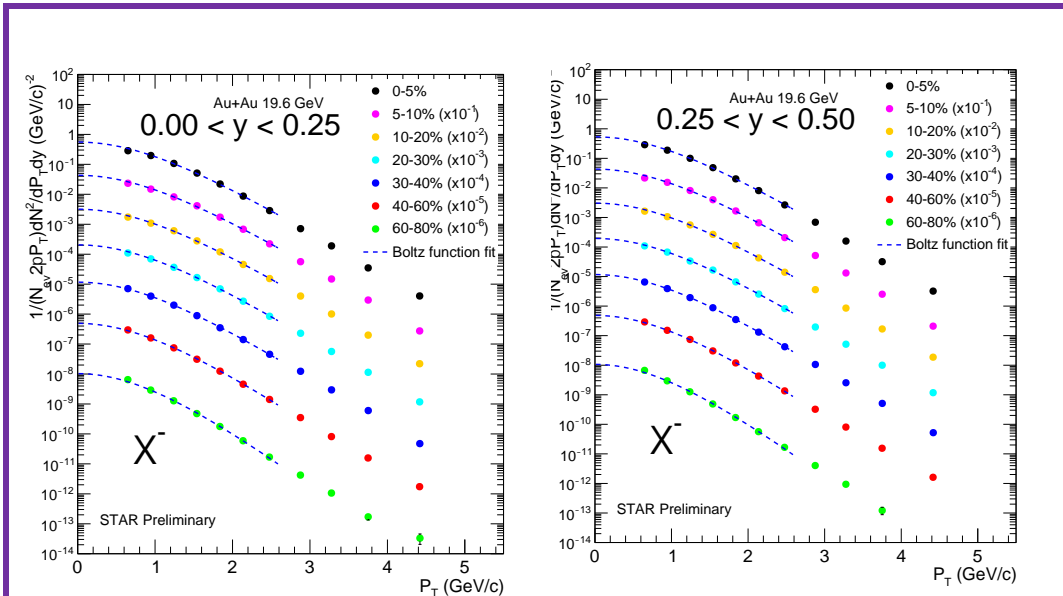
p_T spectra of K_S^0 and Λ at 19.6 GeV



- K_S^0 : measured down to $p_T=0$, no need for extrapolation to obtain dN/dy
- Rapidity: $|y| < 1.5$

- Low p_T extrapolation: Boltzmann function
- Corrected for Ξ^- and Ξ^0 feed-down
- Rapidity: $|y| < 1$

p_T spectra of Ξ^- , ϕ and $\Omega^- (\bar{\Omega}^+)$ at 19.6 GeV

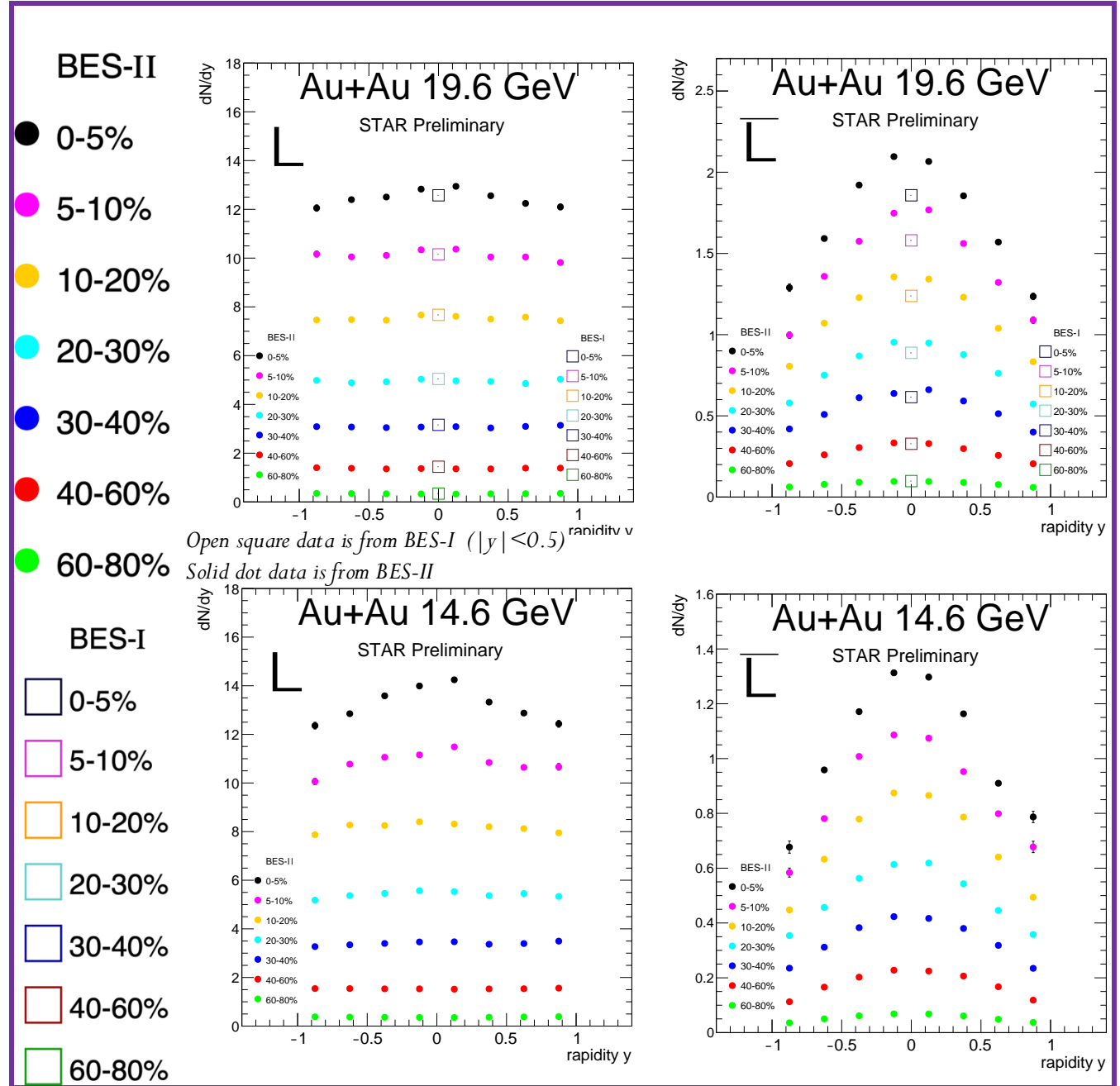


- Ξ^- Low p_T extrapolation: Boltzmann function
- Rapidity: $|y| < 1.0$
- Ω low p_T extrapolation: Boltzmann function
- Rapidity: $|y| < 0.5$
- ϕ low p_T extrapolation: Levy function
- Rapidity: $|y| < 0.5$

Rapidity spectra of $\Lambda(\bar{\Lambda})$ at 19.6 and 14.6 GeV

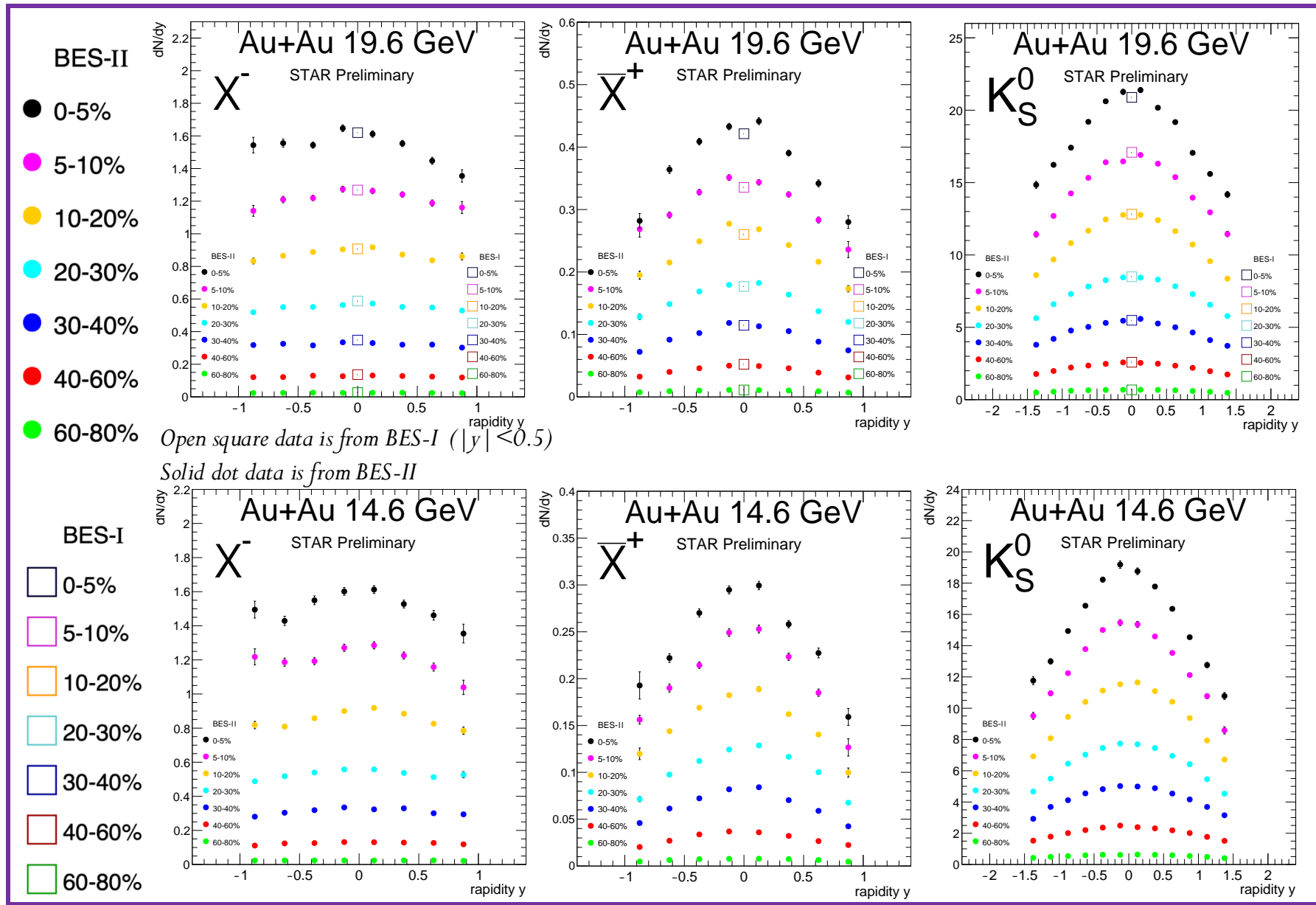
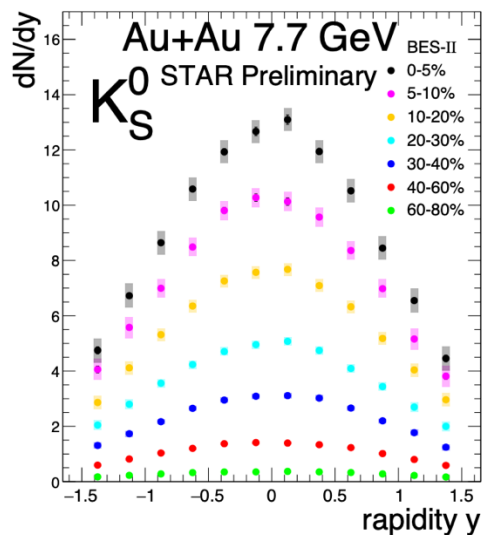
- Rapidity spectra of anti-baryons($\bar{\Lambda}$) are Gaussian-like distributions.
- Rapidity distribution of baryons(Λ) are wider than that of anti-baryons ($\bar{\Lambda}$).
 - ✓ Extra contributions from stopped baryons
- Similar trends observed by NA49.

NA49, PRC 78, 034918 (2008)

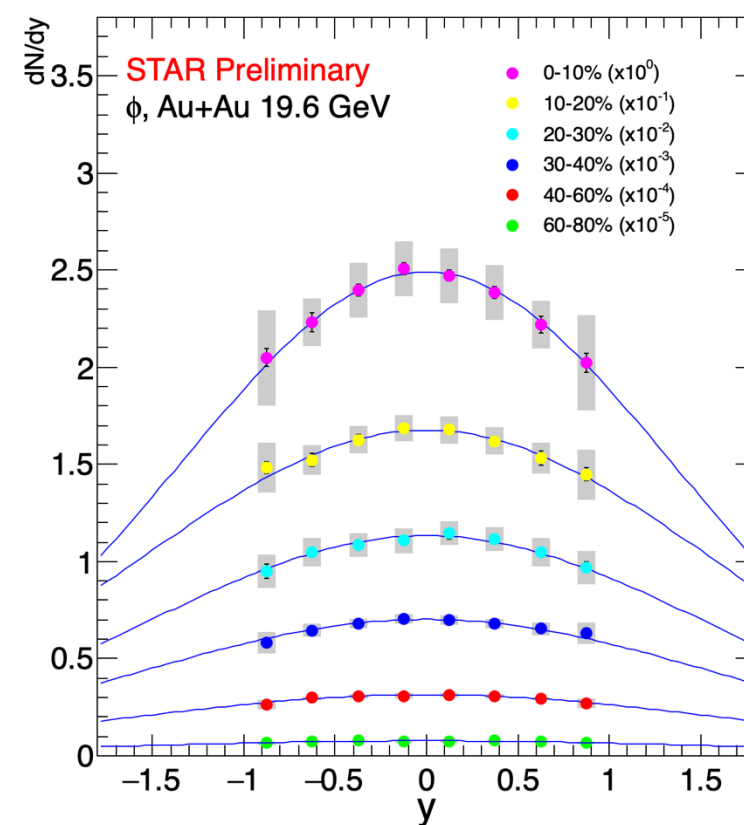
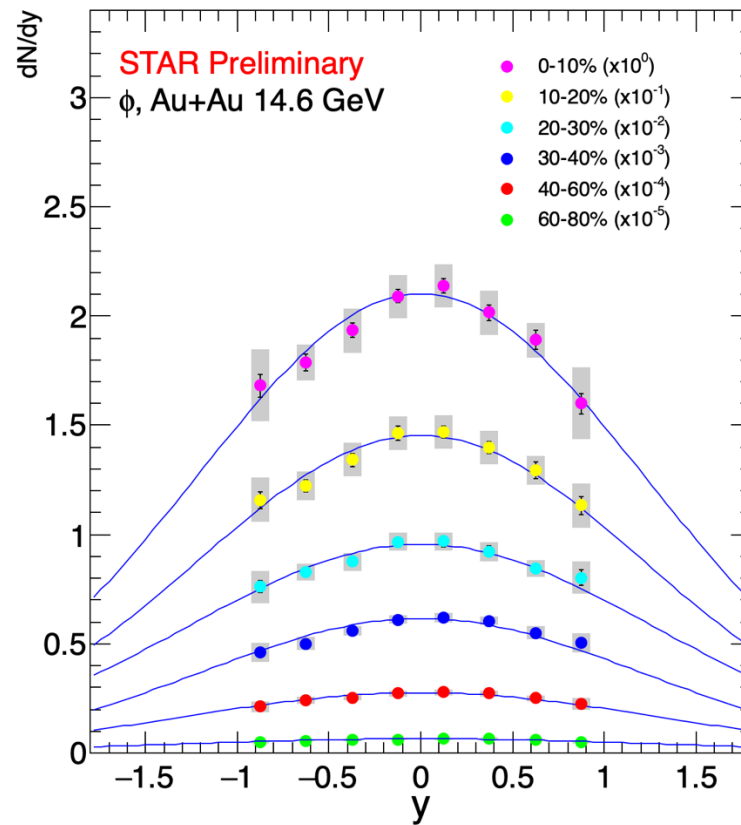
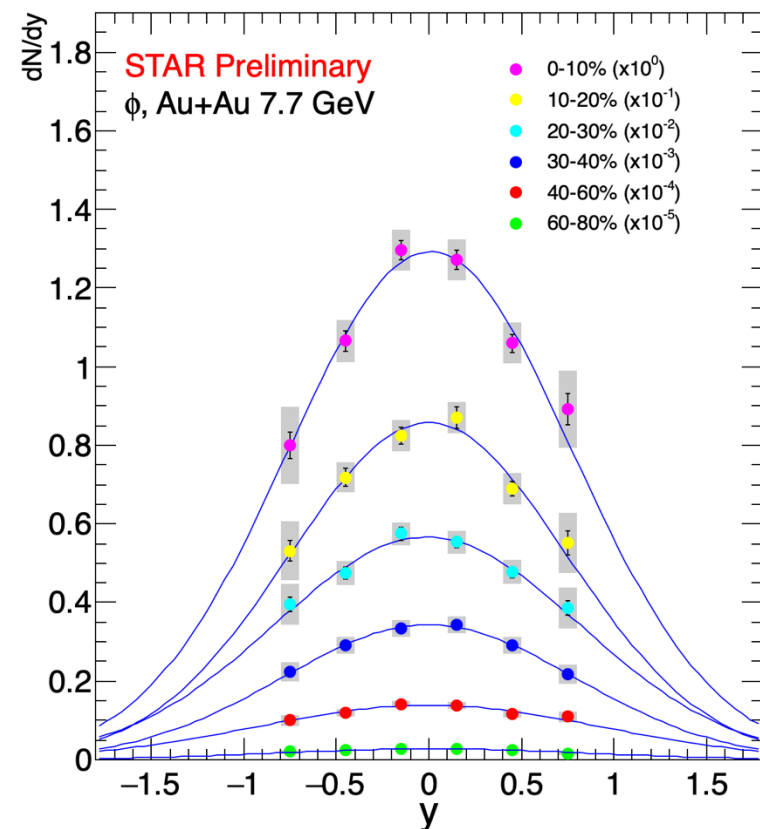


Rapidity spectra of K_S^0 , Ξ^- and Ξ^+ at 19.6 and 14.6 GeV

- Rapidity spectra of mesons (K_S^0) and anti-baryons (Ξ^+) are Gaussian-like distributions.
- Rapidity distribution of baryons (Ξ^-) are wider than the distributions of the anti-baryons (Ξ^+) in Au+Au collisions.



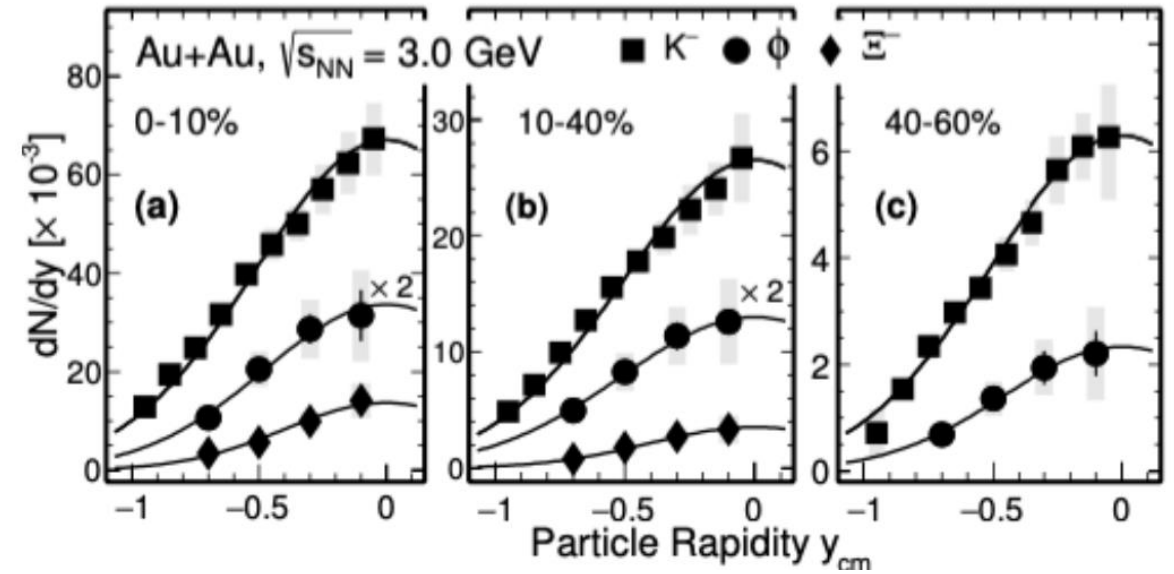
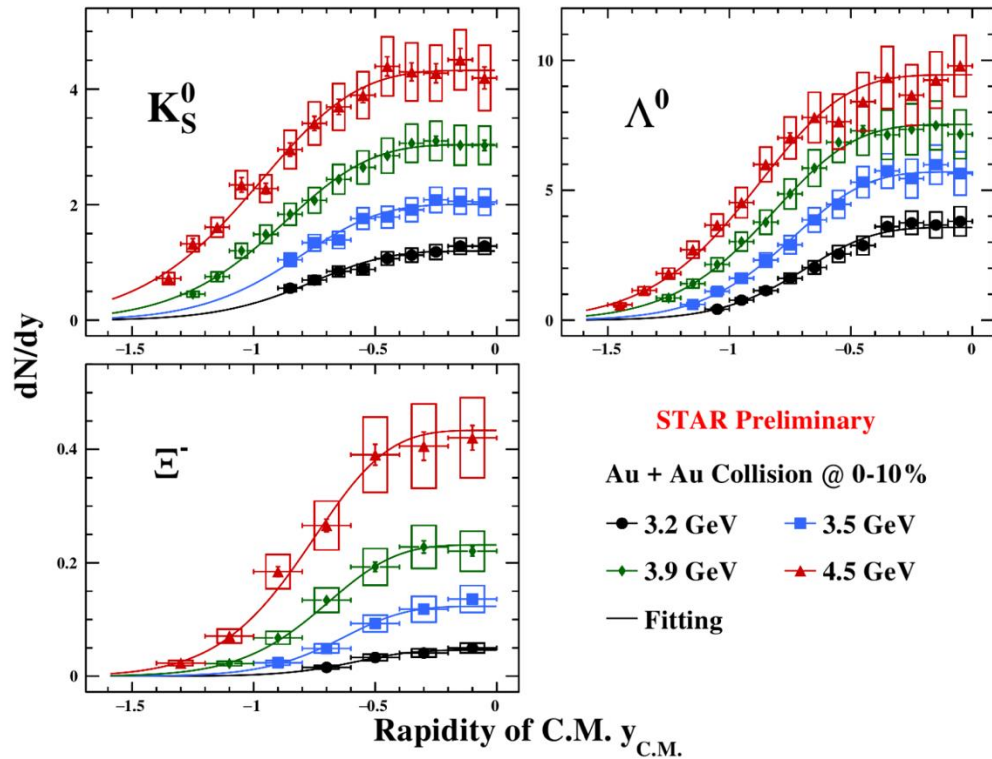
Rapidity spectra of ϕ



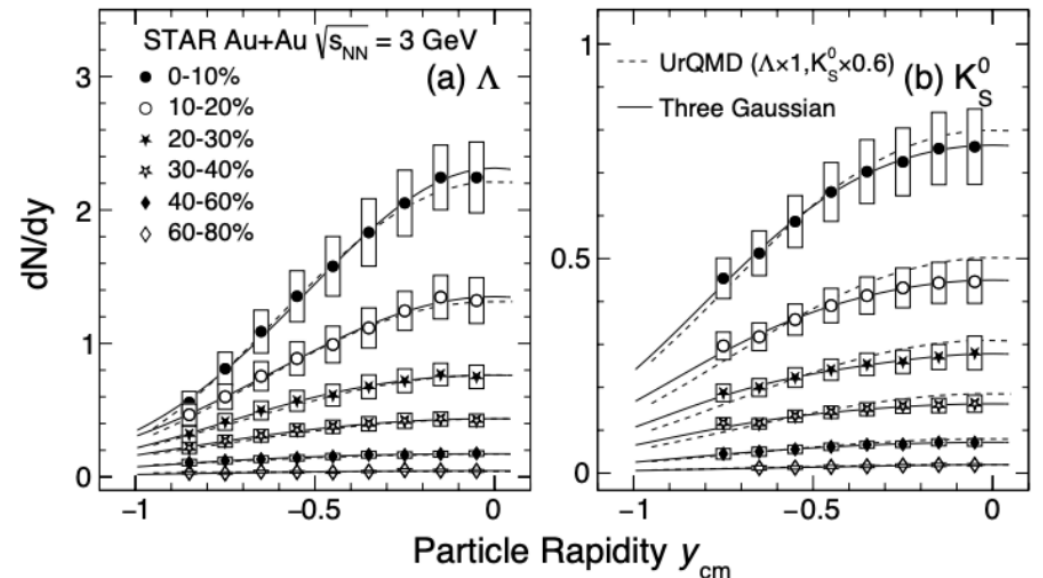
- Rapidity spectra of ϕ are **Gaussian-like** distributions
- Rapidity distribution **become wider with increasing energy**

Rapidity spectra of K^- , K_S^0 , ϕ , Λ and Ξ^- at 3.0-4.5 GeV (FXT)

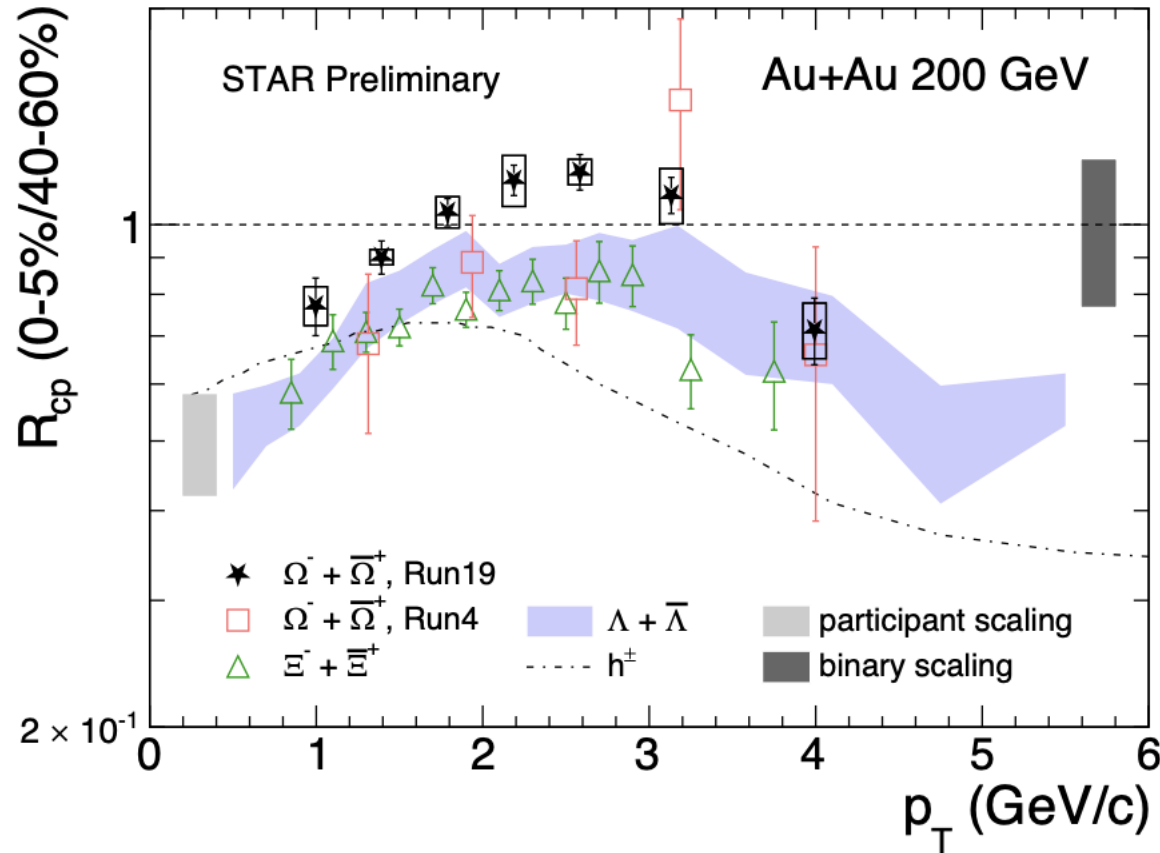
STAR: Phys. Lett. B 831 (2022) 137152; arXiv: 2407.10110



- Comprehensive measurement of strangeness production at different energies from 3 to 4.5 GeV



R_{CP} of strange hadrons at 200 GeV



$$R_{CP} = \frac{[(dN/dp_T)/\langle N_{coll} \rangle]_{\text{central}}}{[(dN/dp_T)/\langle N_{coll} \rangle]_{\text{peripheral}}}$$

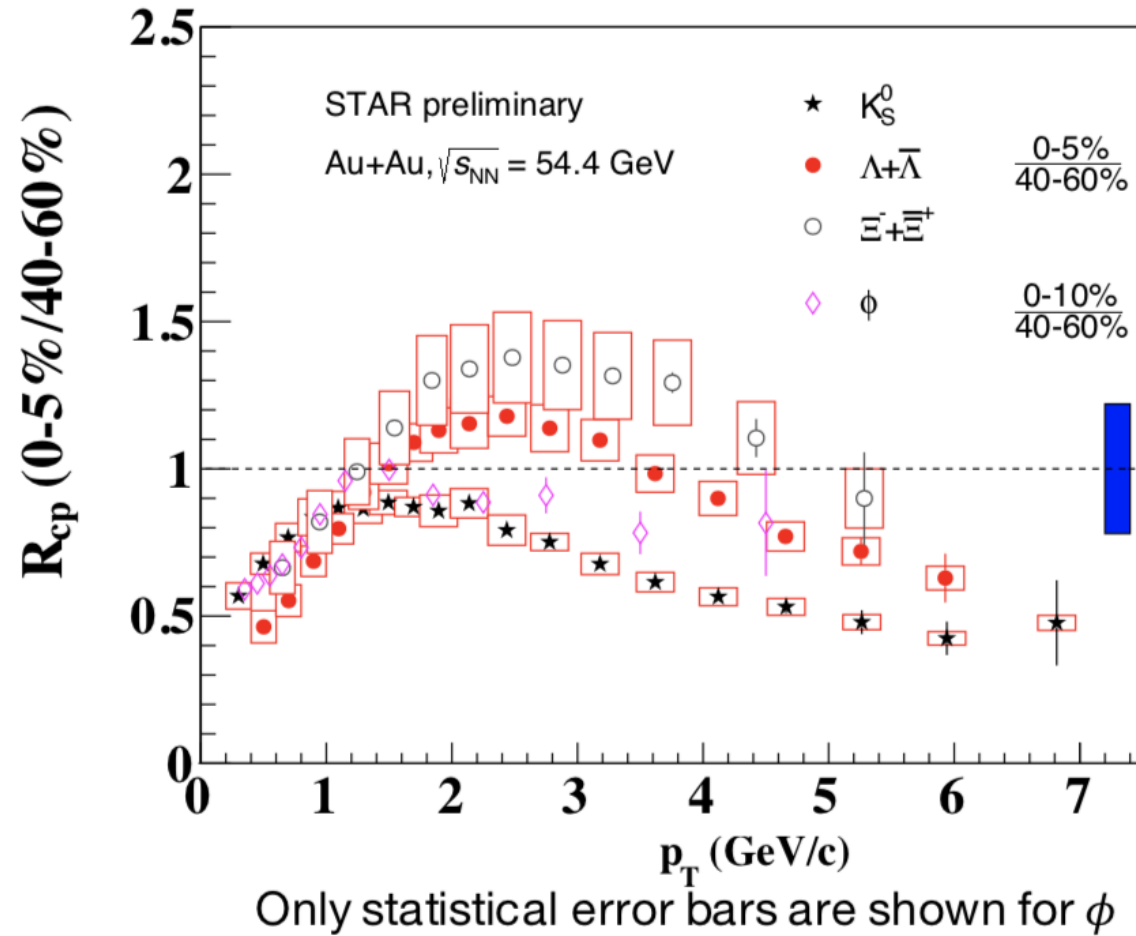
- R_{cp} of Ω follows the same trend in p_T as that of Λ and Ξ , as expected from recombination model.
- The higher R_{cp} of Ω implies the faster increase of Ω yields with the increasing centrality.

$\Omega + \bar{\Omega}$ Run4 & $\Xi + \bar{\Xi}$: STAR, Phys. Rev. Lett. 98 (2007) 062301

$\Lambda + \bar{\Lambda}$: STAR, Phys. Rev. Lett. 92 (2004) 052302

h^\pm (charged hadrons): STAR, Phys. Rev. Lett. 91 (2003) 172302

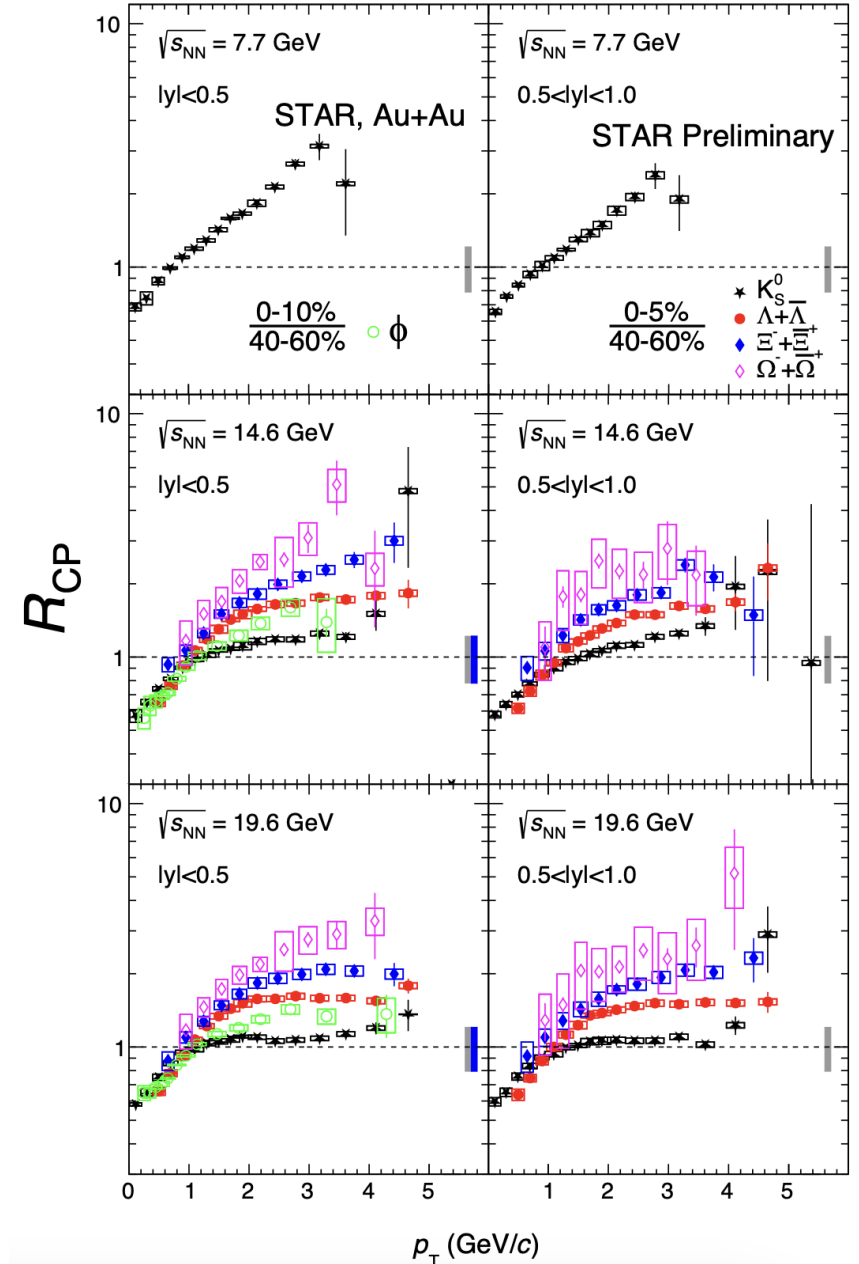
Nuclear modification factor for strange hadrons at 54.4 GeV



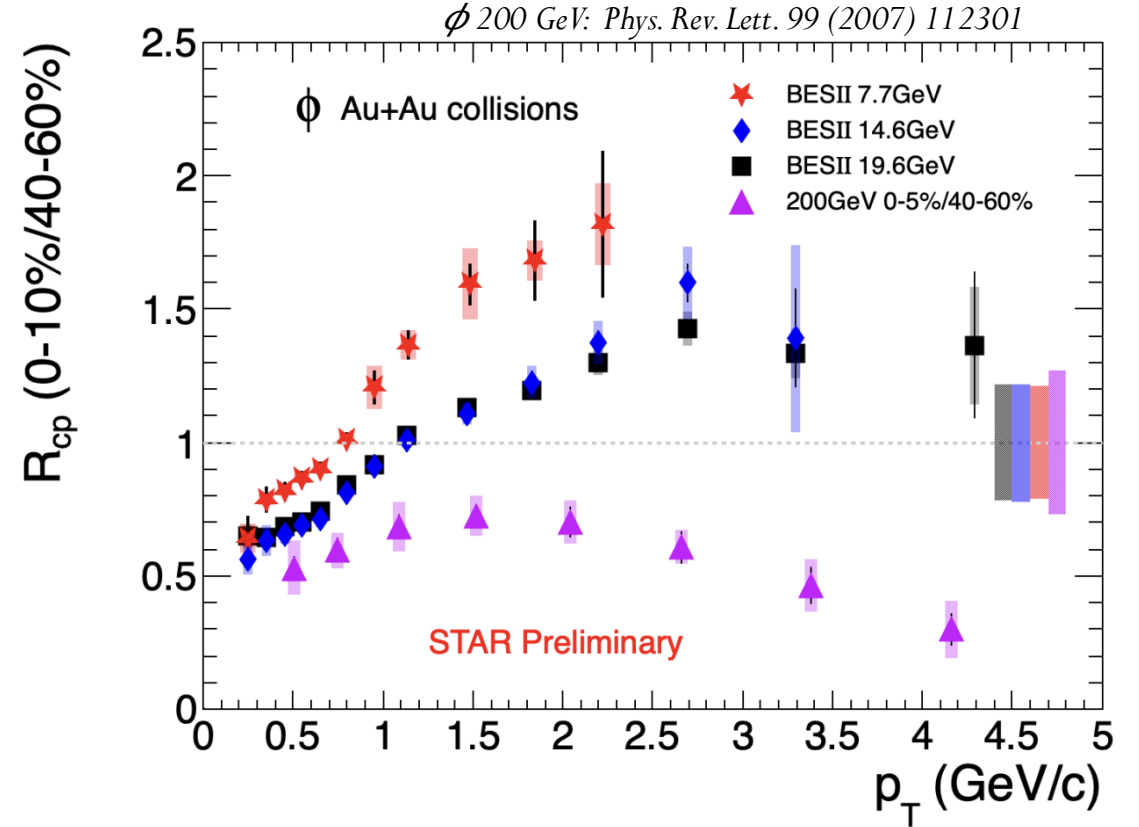
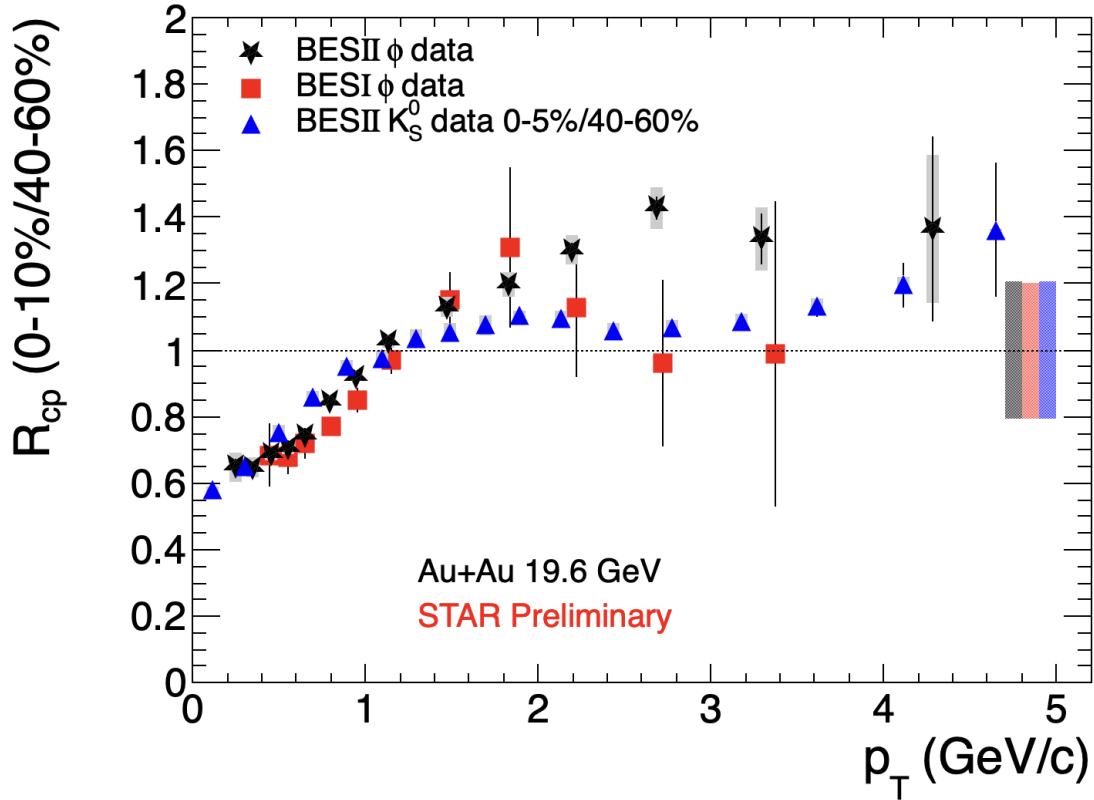
- Strong suppression of $K_S^0 R_{CP}$ at high p_T
→ partonic energy loss

Nuclear modification factor at 19.6, 14.6 and 7.7 GeV

- R_{CP} of K_S^0 increases with decreasing collision energies at $p_T > 2 \text{ GeV}/c$:
 - ✓ Partonic energy loss less important
 - ✓ Cold nuclear matter effect more important
- R_{CP} tends to be flat and larger than unity at $p_T > 2 \text{ GeV}/c$.
 - ✓ Radial flow
 - ✓ Quark coalescence
- The enhancement is stronger for Ω compare to Ξ , Λ and K_S^0
 - ✓ A stronger enhancement for multi-strange particles is a proposed signature for QGP formation.

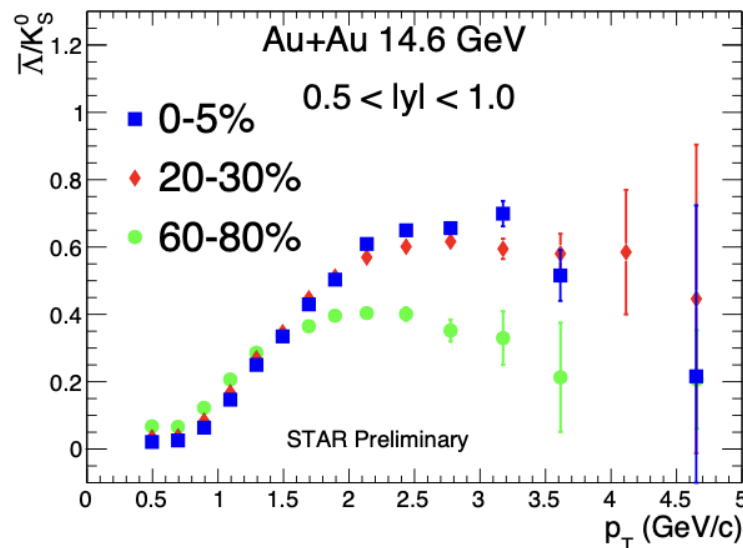
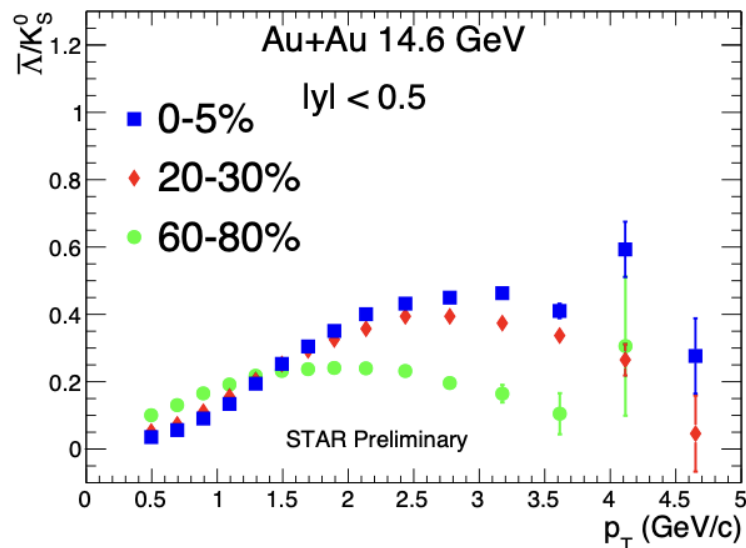
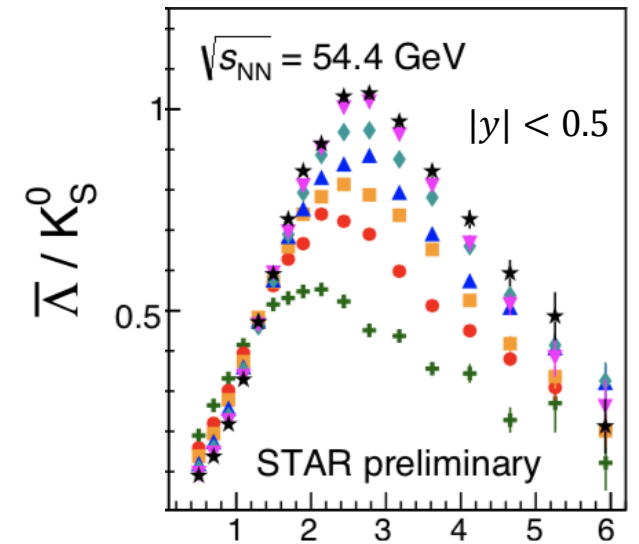
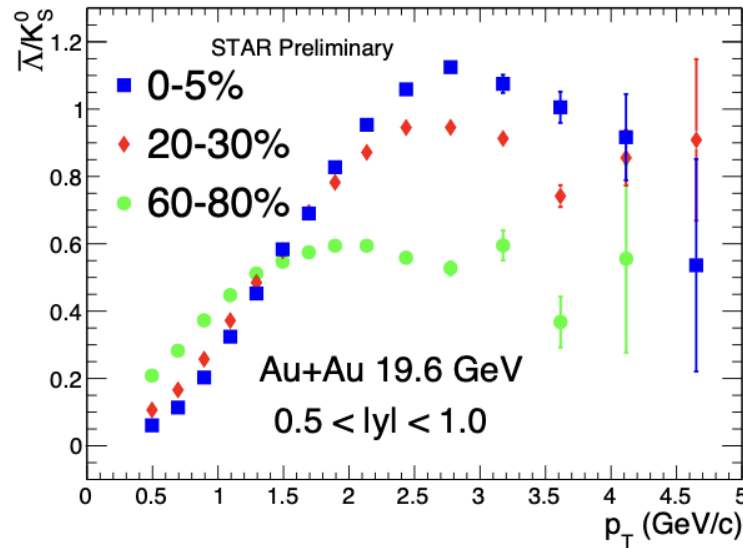
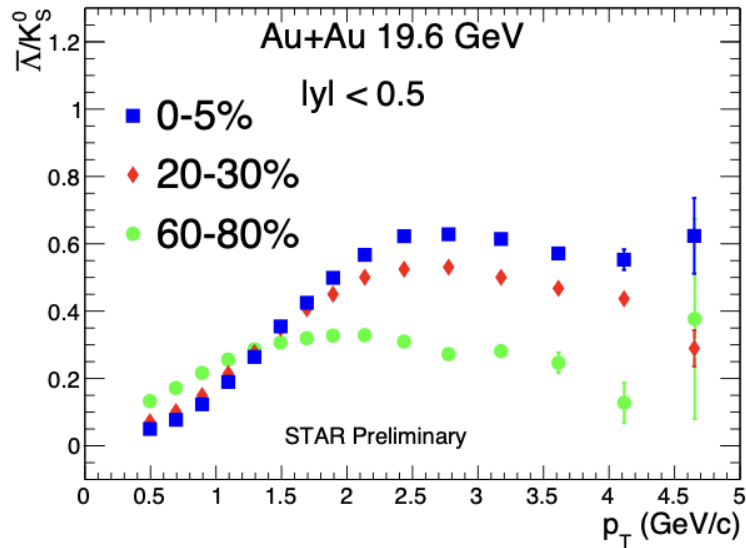


Nuclear modification factor for ϕ



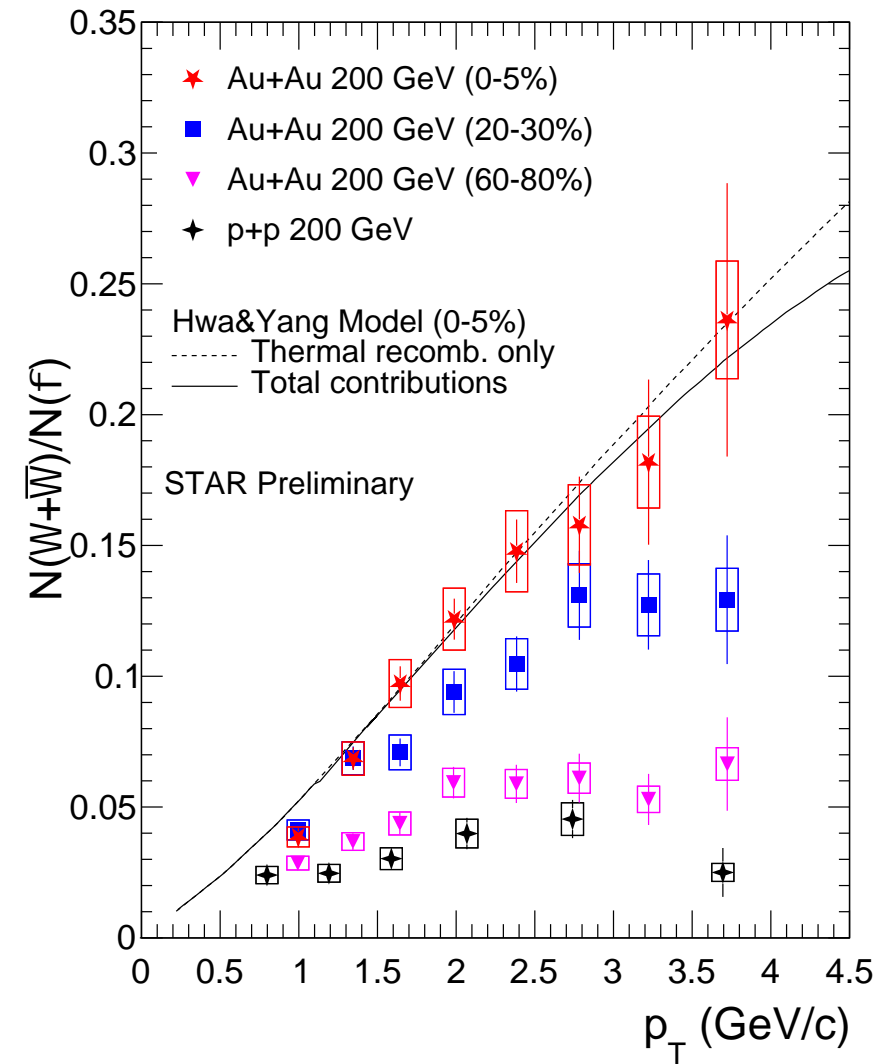
- BES-II result is consistent with BES-I with greatly improved precision
- $R_{CP}(\phi) > R_{CP}(K_S^0)$ at $2 < p_T < 4$ GeV/c
- $R_{CP} < 1$ for higher p_T at 200 GeV \rightarrow Partonic energy loss in the QGP medium
- $R_{CP} > 1$ for higher p_T at 19.6 GeV and lower energies \rightarrow Cronin-type interactions, radial flow and/or coalescence hadronization

$\bar{\Lambda}/K_S^0$ ratio at 54.4, 19.6 and 14.6 GeV



- Clear centrality and rapidity dependence of (anti-)baryon-to-meson ratio at intermediate p_T .
- Baryon enhancement is observed in all measured rapidity regions.

$\Omega(sss)/\phi(s\bar{s})$ ratio at 200 GeV



- In central collisions, good agreement between data and recombination model calculations.
 - ✓ Ω and ϕ are predominantly produced through the recombination of thermalized strange quarks in QGP.
- At intermediate p_T , ratio increases gradually with increasing system size. Significant Ω enhancement over ϕ is observed.
- Ω/ϕ ratio in p+p collisions is close to that in peripheral Au+Au collisions.
 - ✓ Hint of smooth transition from p+p collisions to Au+Au collisions.

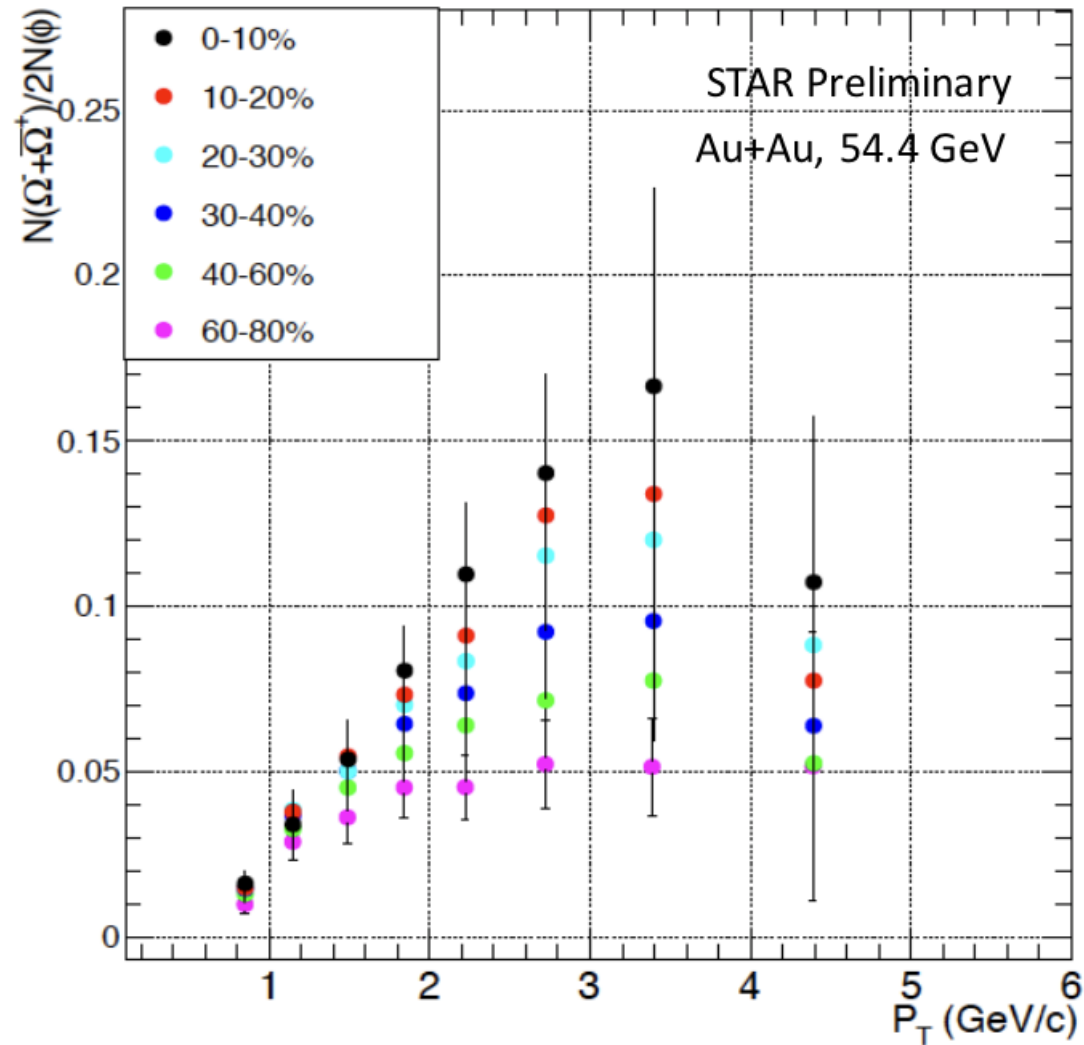
Ω p_T binning adapted to match ϕ data.

Au+Au 200 GeV ϕ : STAR, Phys. Rev. Lett. 99(2007) 112301

p+p 200GeV $\Omega + \bar{\Omega}$: X. Zhu, QM2014; p+p 200GeV ϕ : STAR, Phys. Rev. C 79(2009) 064903

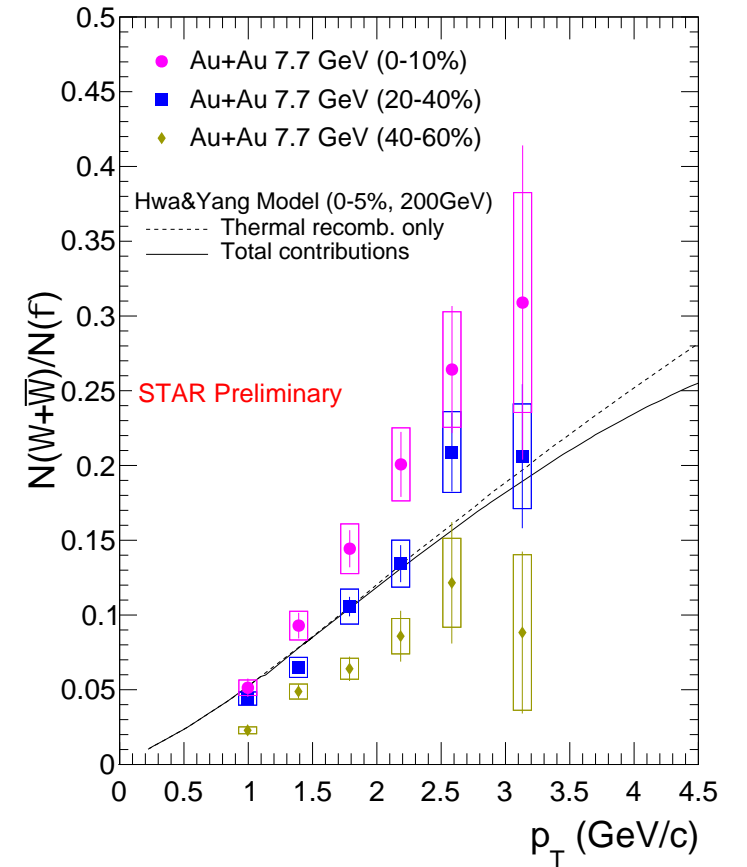
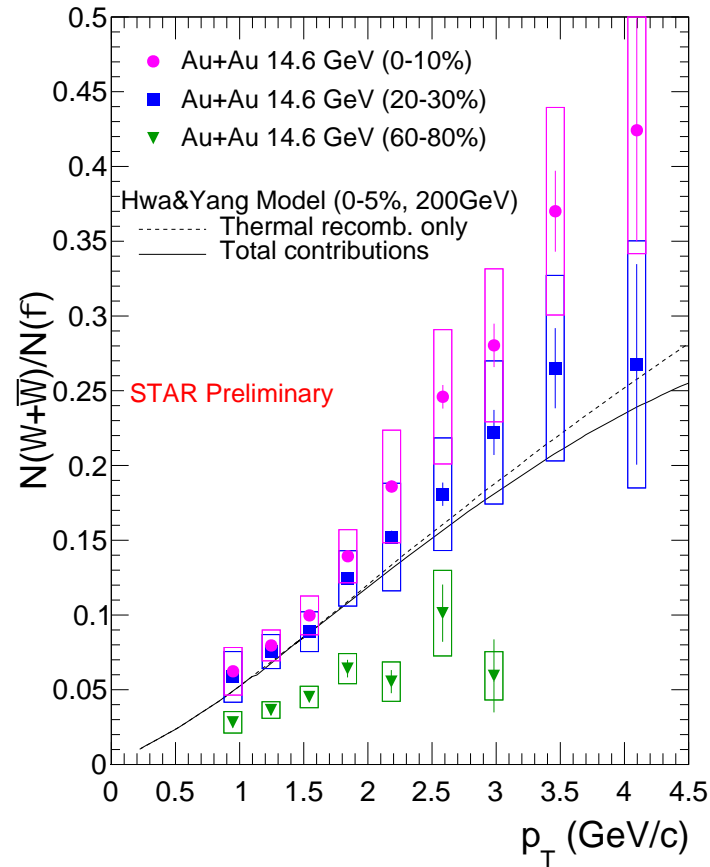
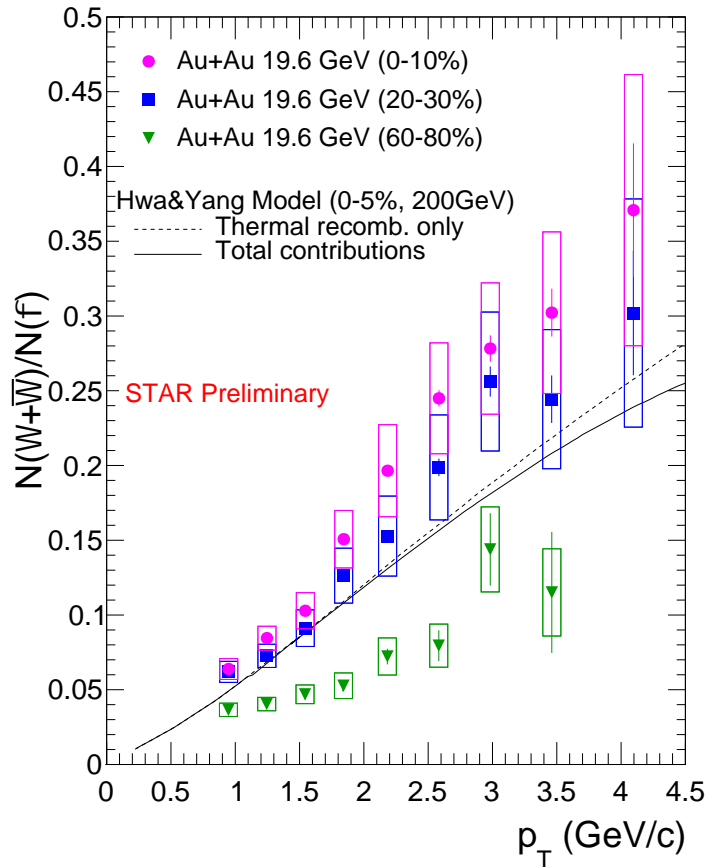
Theory: Phys. Rev. C, 2007, 75: 054904. theoretical calculation only for central collisions

Ω/ϕ ratio at 54.4 GeV



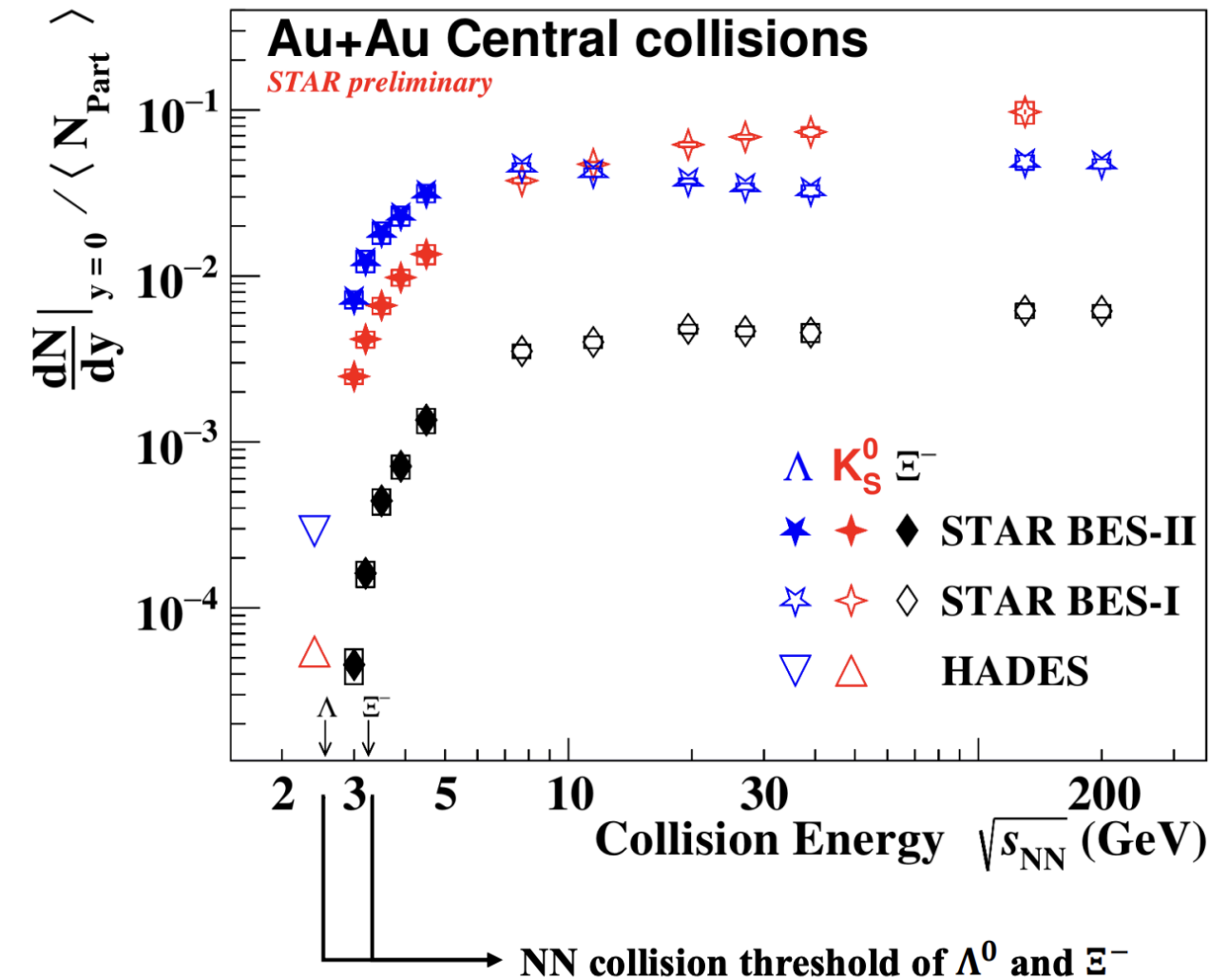
Ω/ϕ ratio enhancement at 54.4 GeV
→ Hadron formation through parton recombination

Ω/ϕ ratio in 19.6, 14.6 and 7.7 GeV



- Similar to the observation at $\sqrt{s_{NN}} = 200$ GeV, the Ω/ϕ ratio increases from peripheral to central collisions at intermediated p_T , which is **compatible with the existence of QGP at $\sqrt{s_{NN}} \geq 7.7$ GeV**

Energy dependence of mid-rapidity yields



- **Rich structure in strangeness excitation functions**

- **Production mechanisms is different at low and high energies (high and low baryon density)**

- **Partonic interaction (pair production)**

$$gg \rightarrow s\bar{s} \text{ or } q\bar{q} \rightarrow s\bar{s}$$

- **Hadronic interaction (associated production)**

$$BB \rightarrow BYK \text{ or } BB \rightarrow BEKK$$

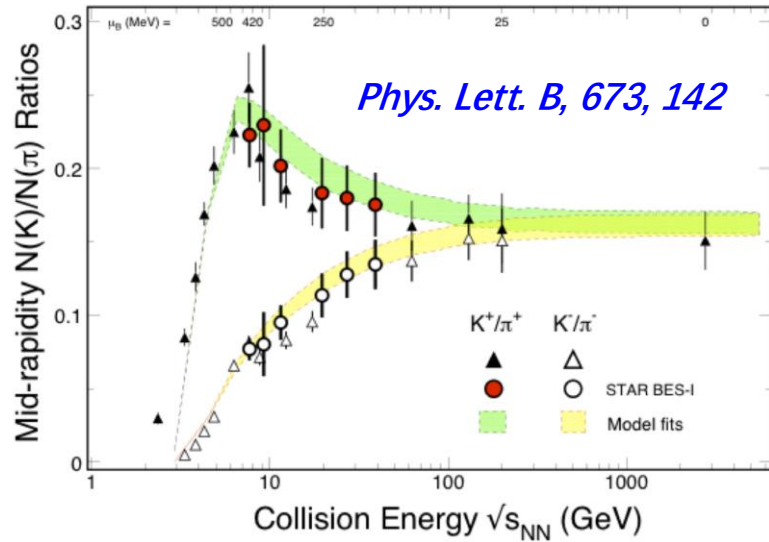
$$B: N, p, \Delta, \text{ etc.} \quad Y: \Lambda, \Sigma, \text{ etc.} \quad K: K^+, K^0$$

- **Baryon-dominated to meson-dominated transitions**

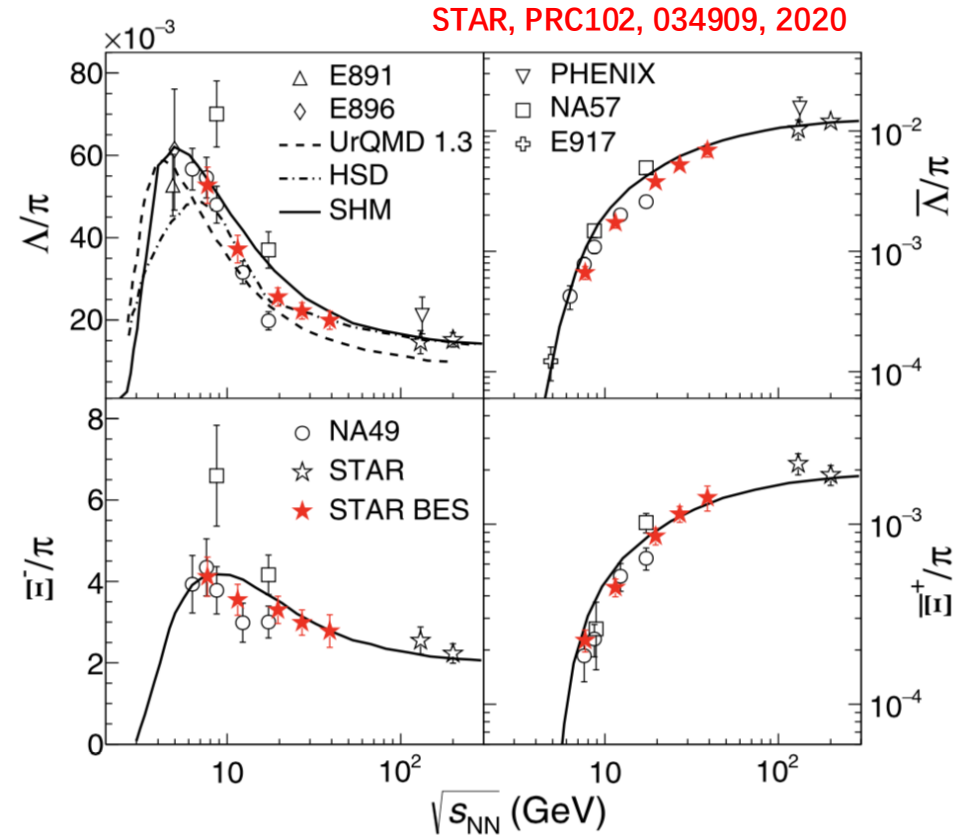
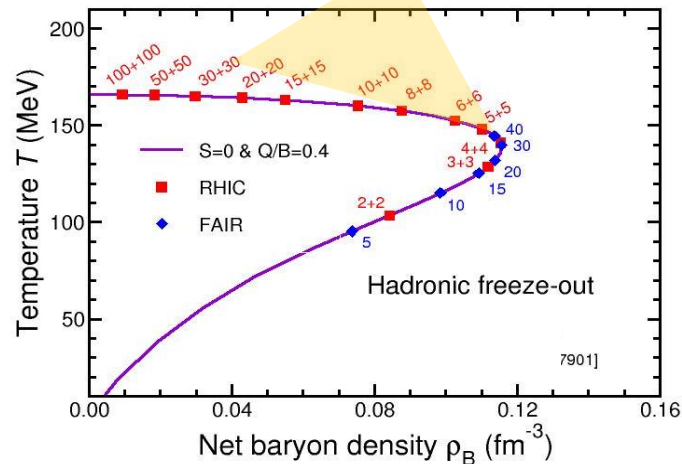
- **K_S^0 and Λ^0 mid-rapidity yield cross at ~ 8 GeV**

- **First measurement of Ξ^- near- / sub-threshold energies in Au+Au collision**

Strange hadron to pion ratio



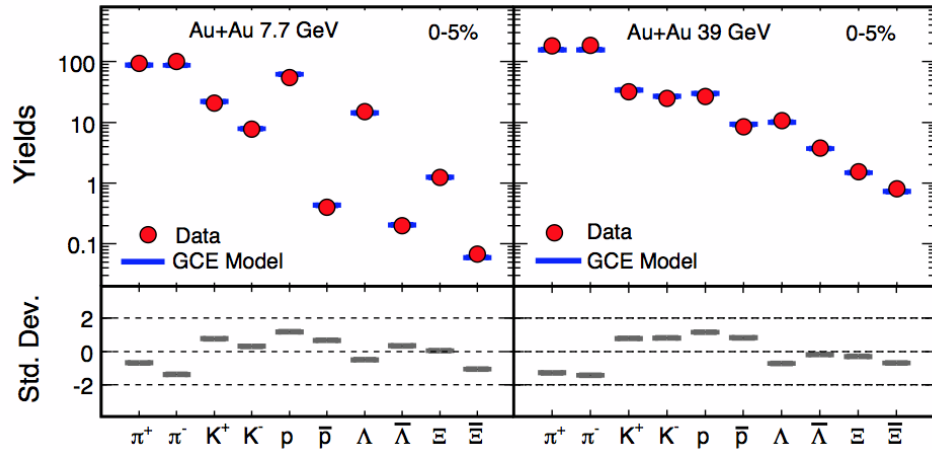
RHIC BES



- Particle ratios consistent with NA49, consistent with the picture of a **maximum net-baryon density around $\sqrt{s_{NN}} \sim 8$ GeV at freeze-out**

Chemical freeze-out parameters: T_{ch} vs. μ_B

STAR, Phys. Rev. C 96, 044904, 2017

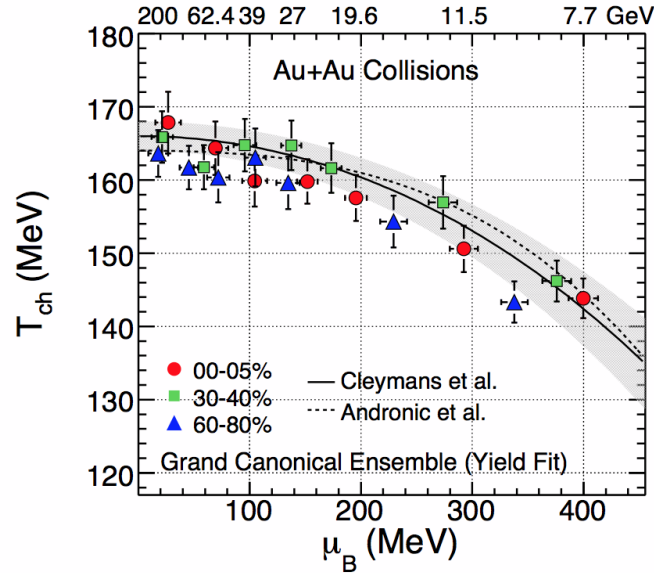


✓ Particles used : π , K , p , Λ , Ξ

✓ Ensemble used:
Grand canonical (GCE)

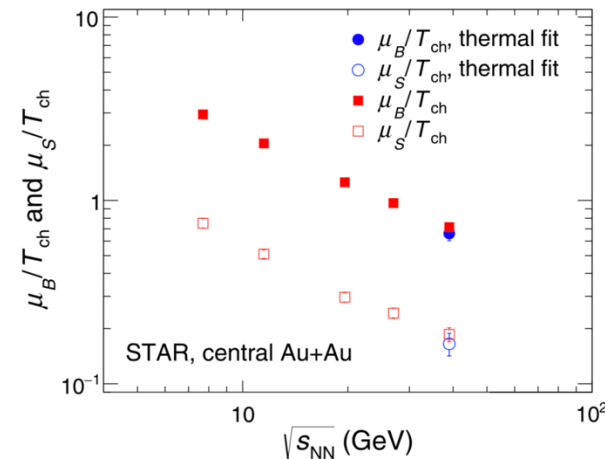
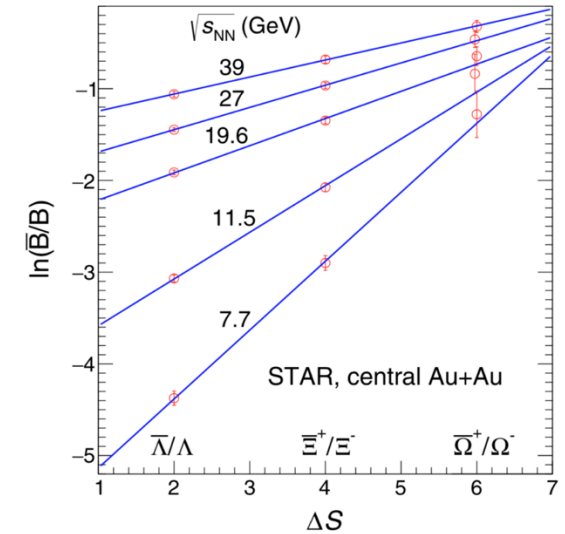
✓ Fit parameters:
 T_{ch} , μ_B , μ_s and γ_s

Thermus, S. Wheaton & J. Cleymans, Comput. Phys. Commun. 180: 84-106, 2009.



Andronic: NPA 834 (2010) 237
Cleymans: PRC 73 (2006) 034905
Au+Au 200 GeV : Phys. Rev. C 83 (2011) 24901

STAR, PRC102, 034909, 2020



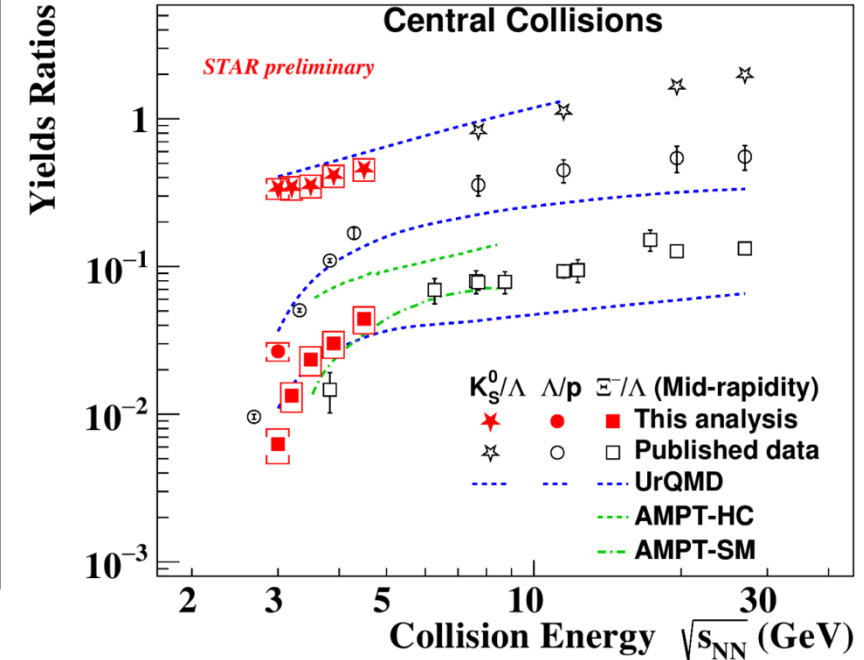
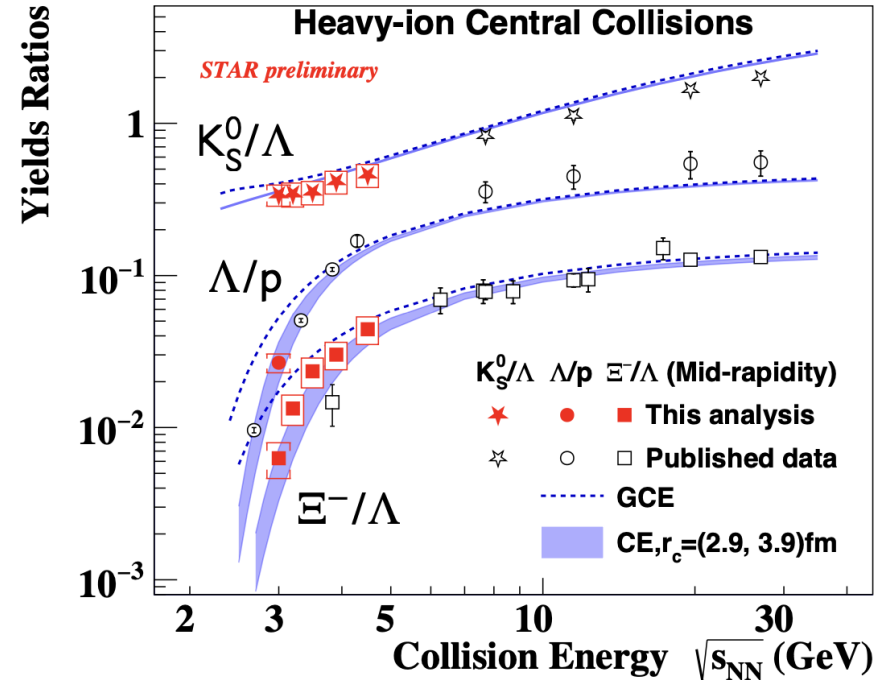
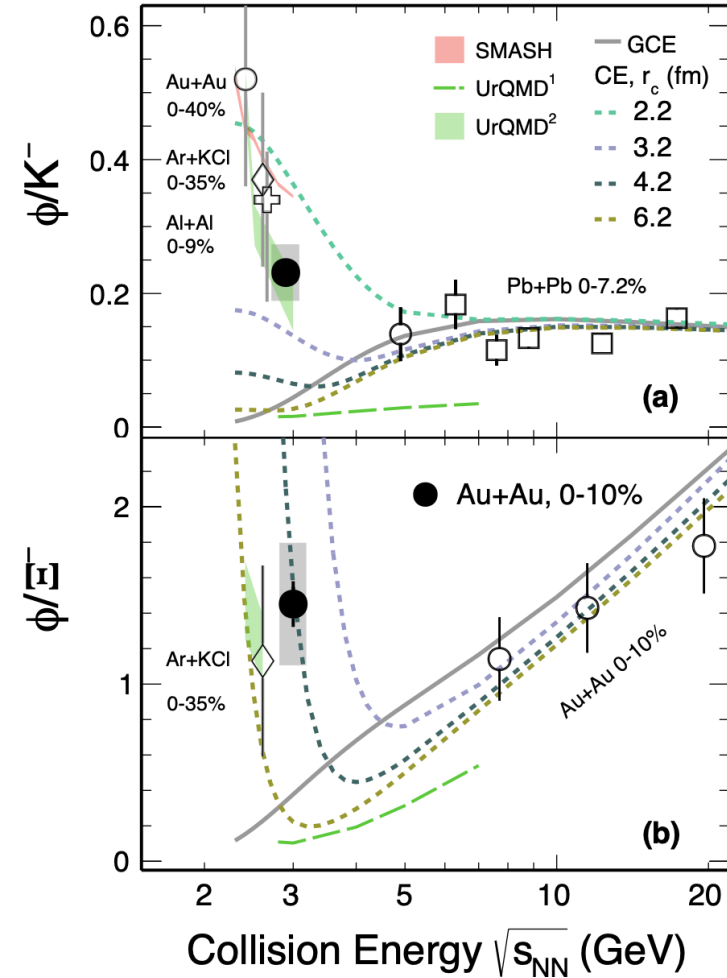
$$\ln\left(\frac{\bar{\Lambda}}{\Lambda}\right) = -\frac{2\mu_B}{T} + \frac{2\mu_S}{T}$$

$$\ln\left(\frac{\bar{\Xi}^+}{\Xi^-}\right) = -\frac{2\mu_B}{T} + \frac{4\mu_S}{T}$$

$$\ln\left(\frac{\bar{\Omega}^+}{\Omega^-}\right) = -\frac{2\mu_B}{T} + \frac{6\mu_S}{T}$$

Energy dependence of mid-rapidity yield ratios

STAR: Phys. Lett. B 831, 137152 (2022)



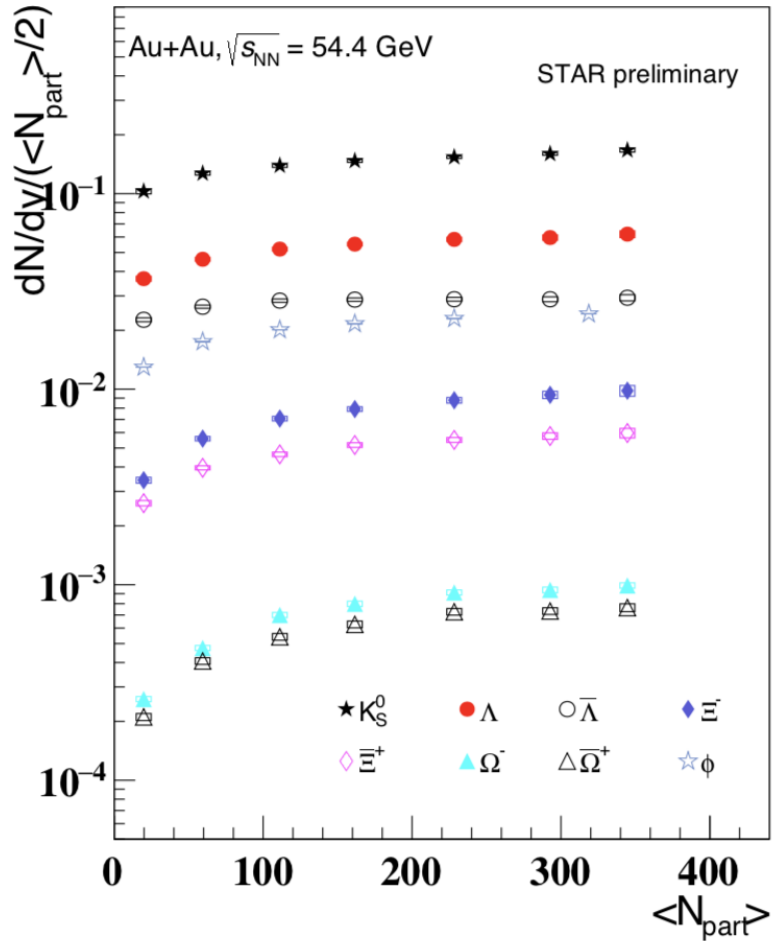
1) Canonical Ensemble (CE) with strangeness correlation length 2.9 – 3.9 fm, simultaneously describes K_S^0/Λ , Λ/p , and E^-/Λ in the measured energy range, GCE fails at low energies

- Similar observations for ϕ/K^- and ϕ/E^-

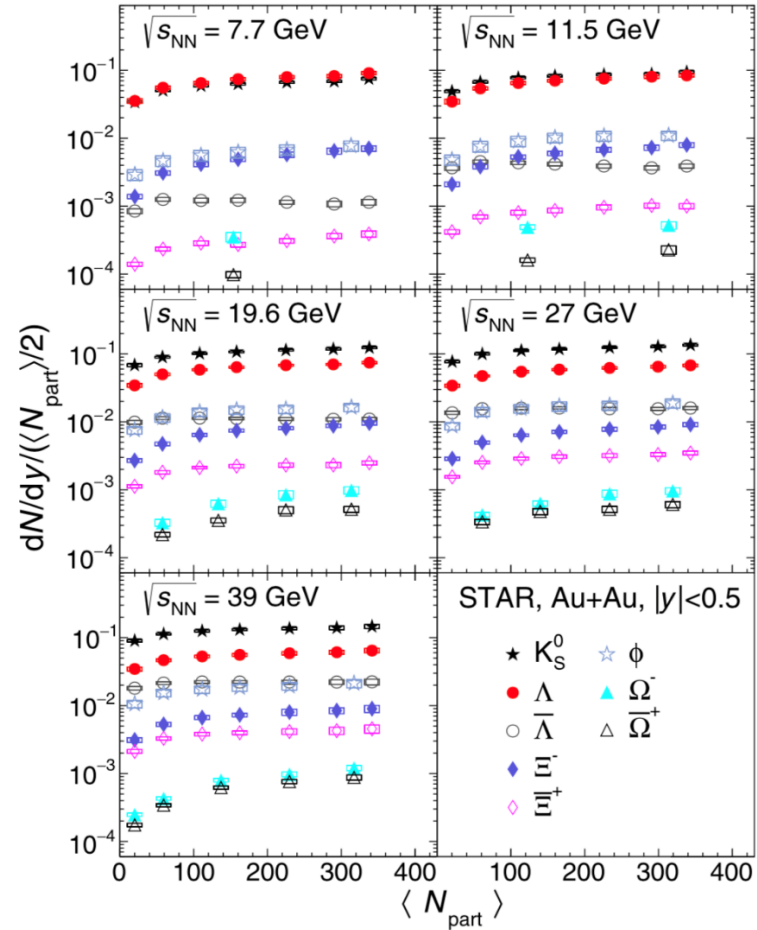
➔ Change of medium properties at the high-density region

UrQMD: cascade mode, hard EOS

Centrality dependence of mid-rapidity yields



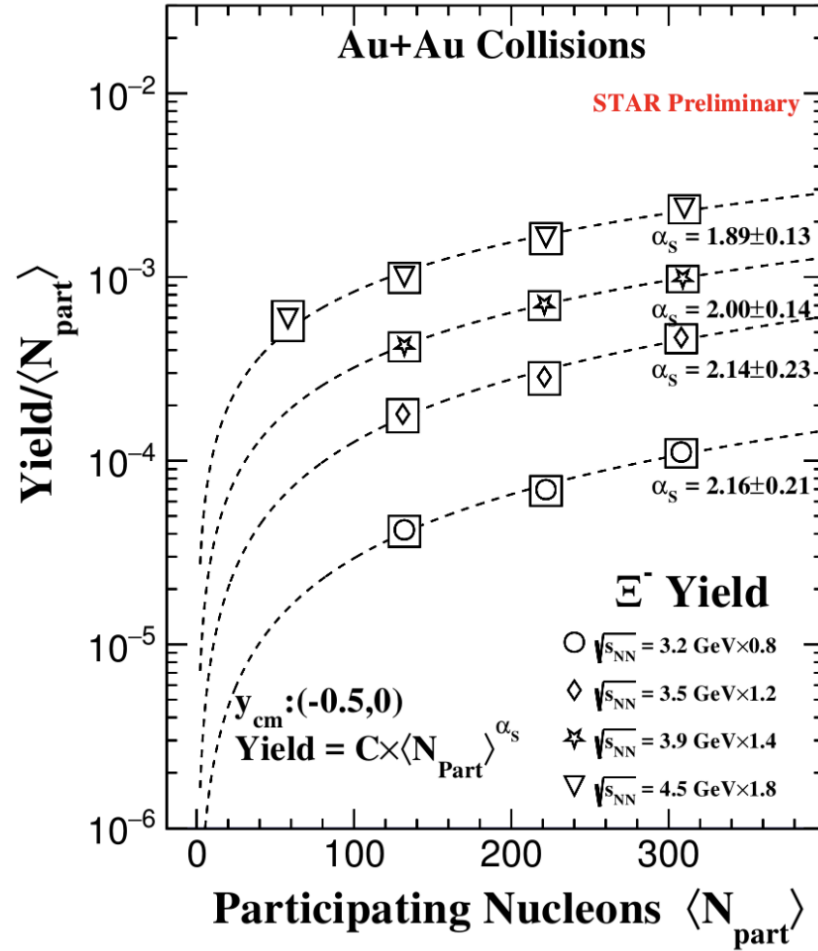
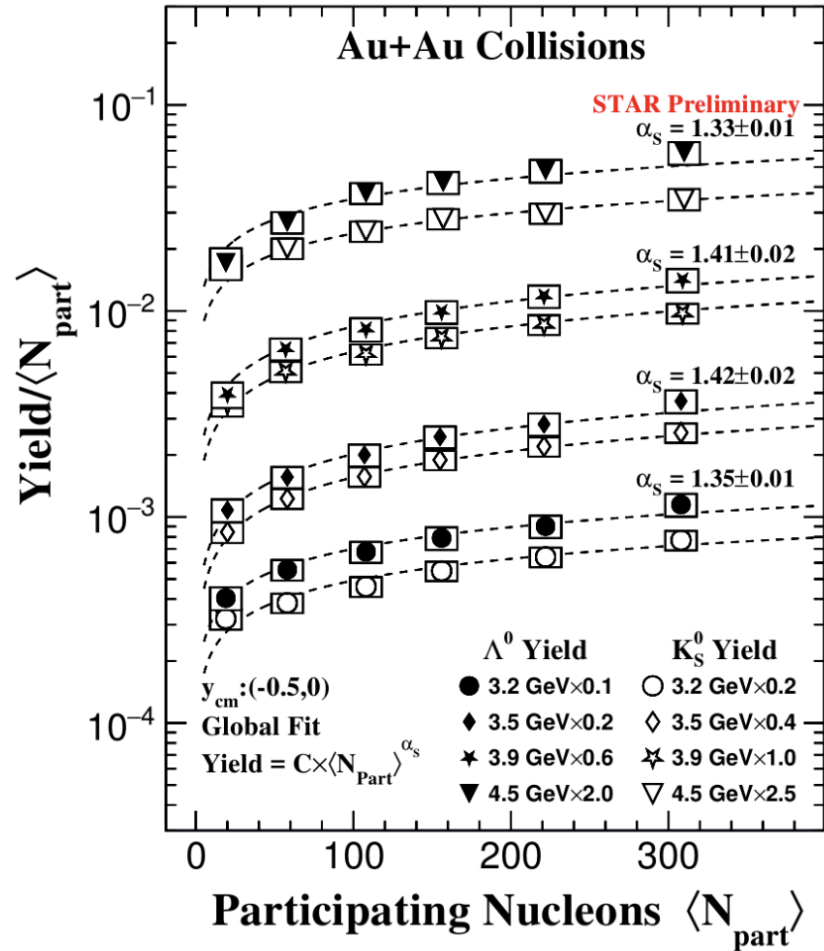
Y. Huang, SQM2021



STAR, PRC102, 034909, 2020

- Yield per participating pair increases towards central and higher energies in general, except that $\bar{\Lambda}$ has weak centrality dependence

Centrality dependence of mid-rapidity yields



- **Scaling formula:**

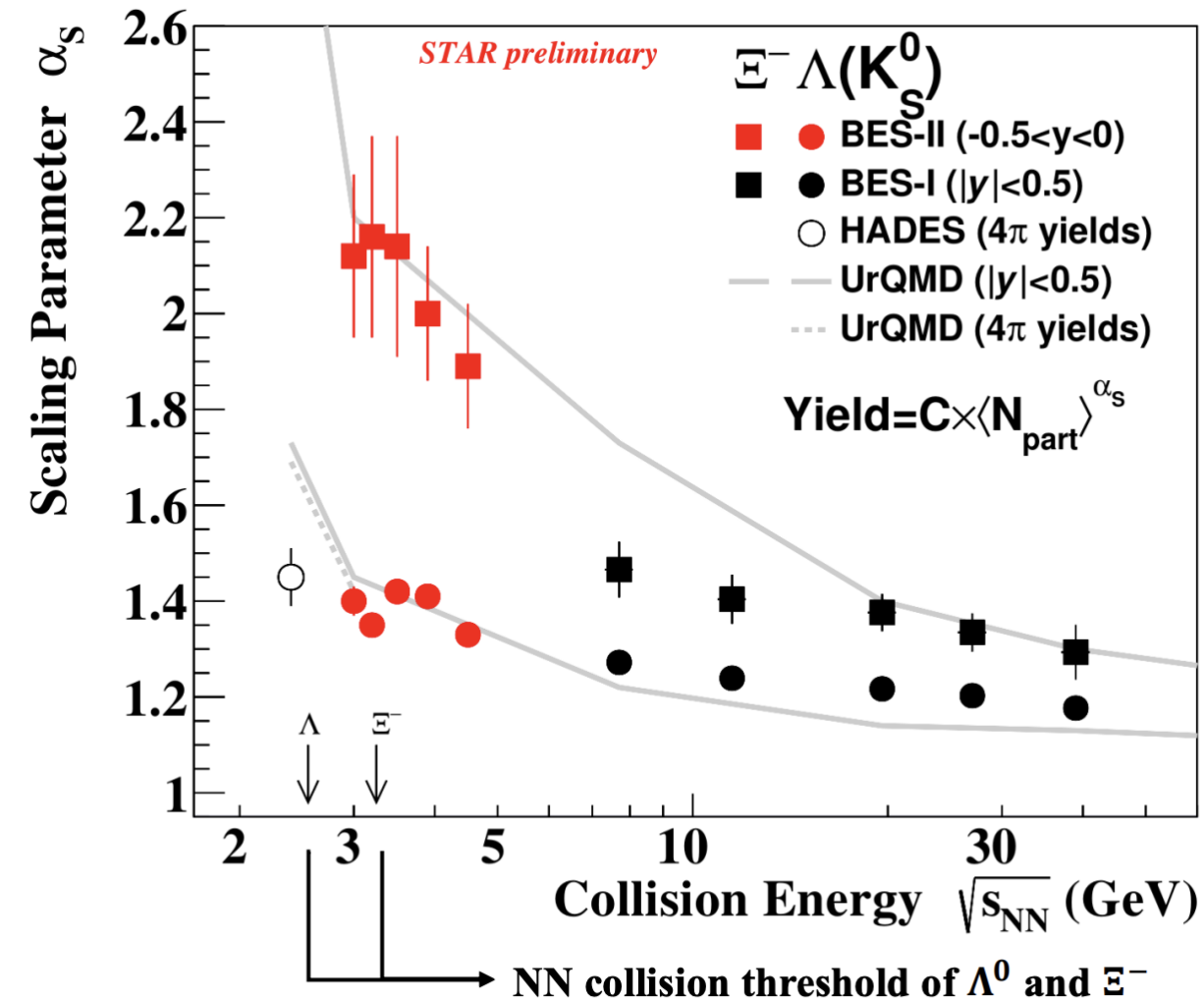
$$\text{Yield} = c \times \langle N_{\text{part}} \rangle^{\alpha_s}$$

- **Single strange hadrons K_S^0 and Λ^0 follow common scaling trend, but double strange hadron Ξ^- deviate from the common scaling trend**

➤ **Associated production mode**

- $\text{NN} \rightarrow \text{N}\Lambda\text{K}$
- $\text{NN} \rightarrow \text{N}\Xi\text{K}$

Energy dependence of scaling parameter α_S

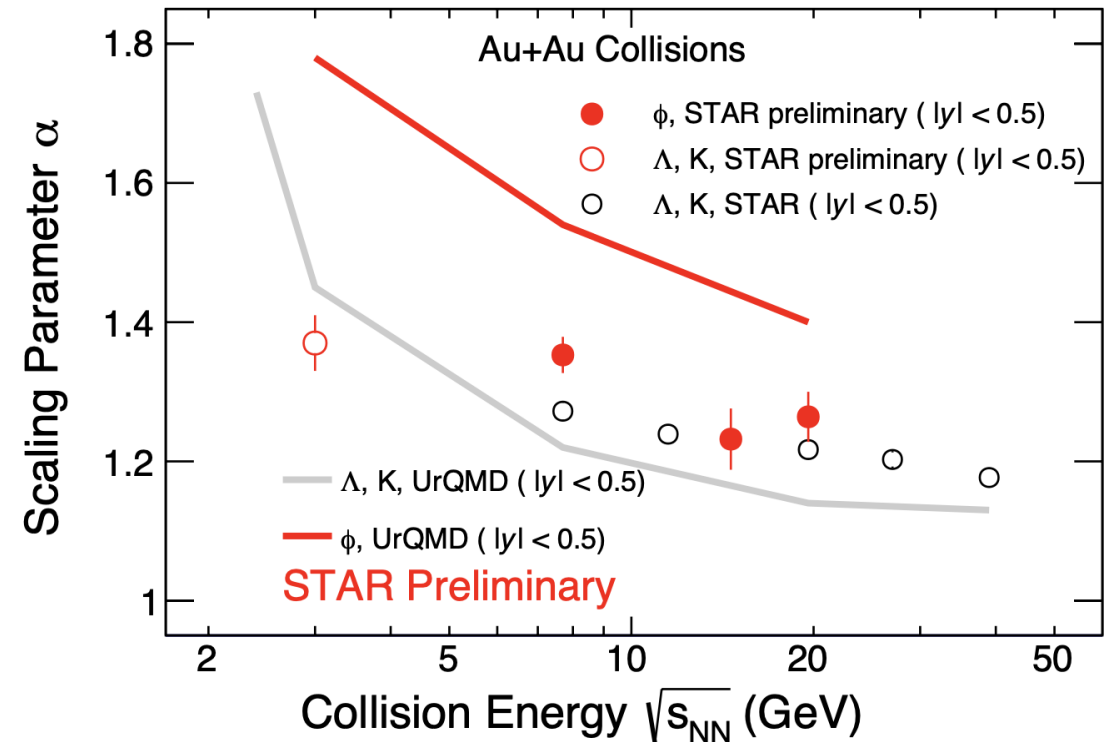
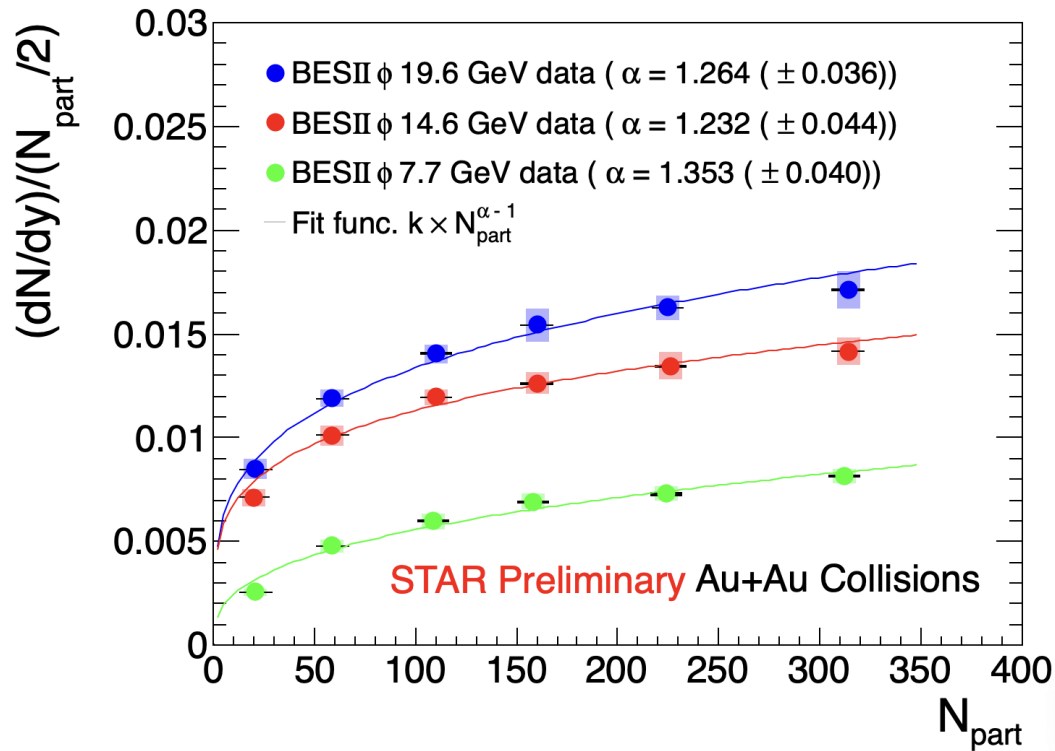


- **Rapid decrease of scaling parameter α_S for E^- from 4.5 to 7.7 GeV, and saturate at high energy**
 - The mechanism of strange hadron production may change
 - Strange hadron production predominantly from hadronic interactions at $\sqrt{s_{NN}} < 4.5$ GeV
- **UrQMD qualitatively reproduces the energy dependence, but cannot quantitatively describe all energies**
 - likely due to missing medium effects

UrQMD: cascade mode, hard EOS

S.A. Bass, et.al. Prog. Part. Nucl. Phys. 41 (1998)

Centrality dependence of ϕ production



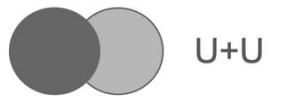
➤ Fit function: $\frac{dN/dy}{N_{\text{part}}/2} = k \times N_{\text{part}}^{\alpha-1}$

➤ Common centrality dependence for ϕ , Λ , K production at 19.6 GeV.

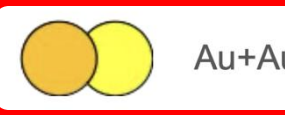
➤ α parameter for ϕ is slightly larger than that for Λ , K and less than UrQMD predictions

STAR: arXiv: 2407.10110

System size dependence of Ω yield at 200 GeV



U+U

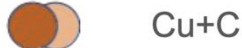


Au+Au

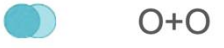


Zr+Zr

Ru+Ru



Cu+Cu



O+O



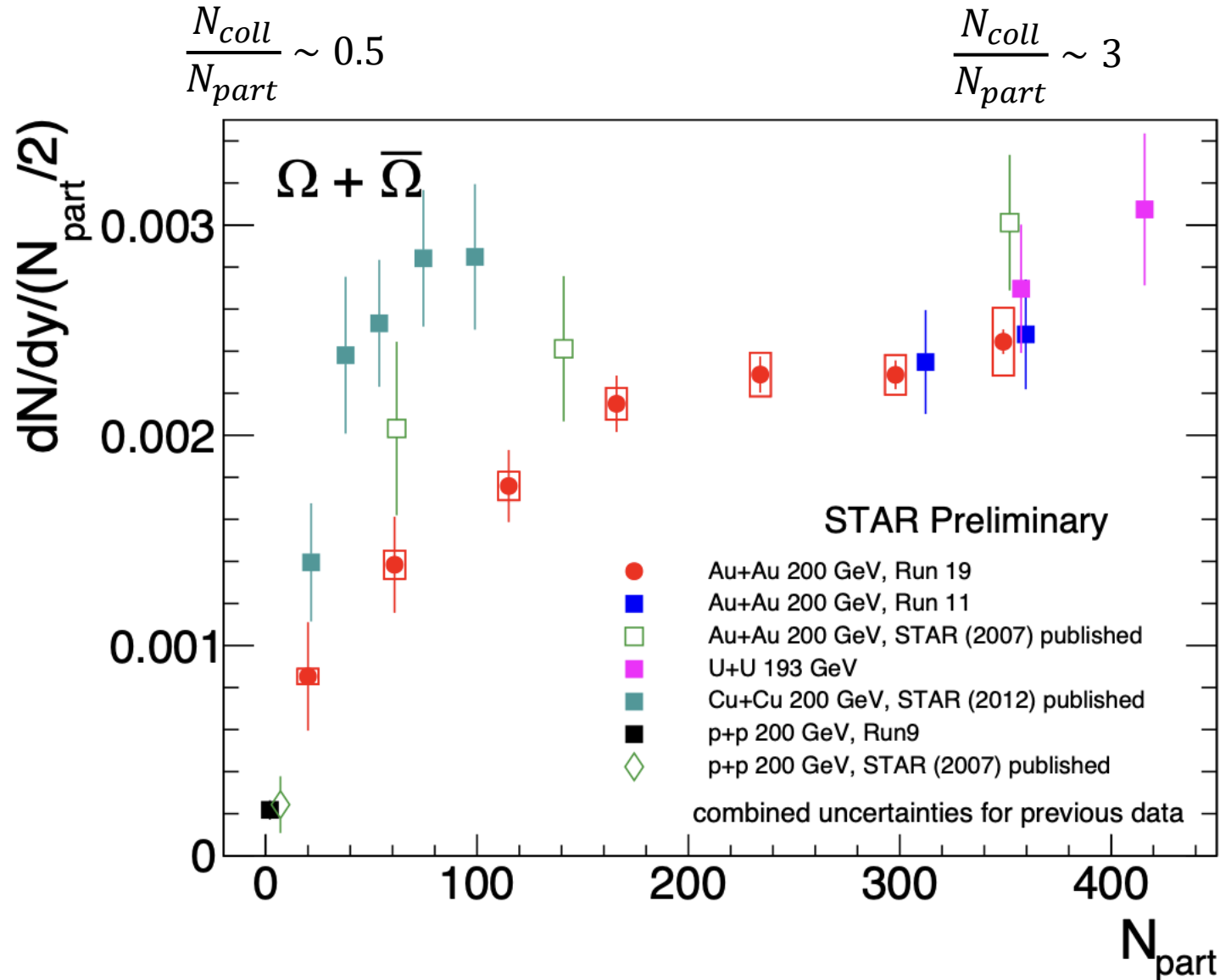
He+Au



d+Au



p+p



➤ In general, increasing Ω baryon enhancement compared to p+p collisions with increasing system size is observed.

➤ Multi-strange hadron production sensitive to multiple collisions.

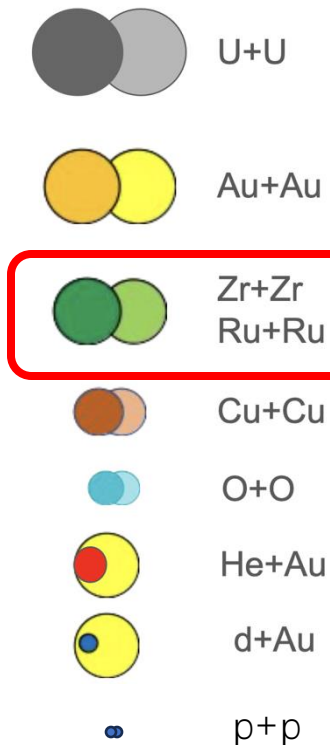
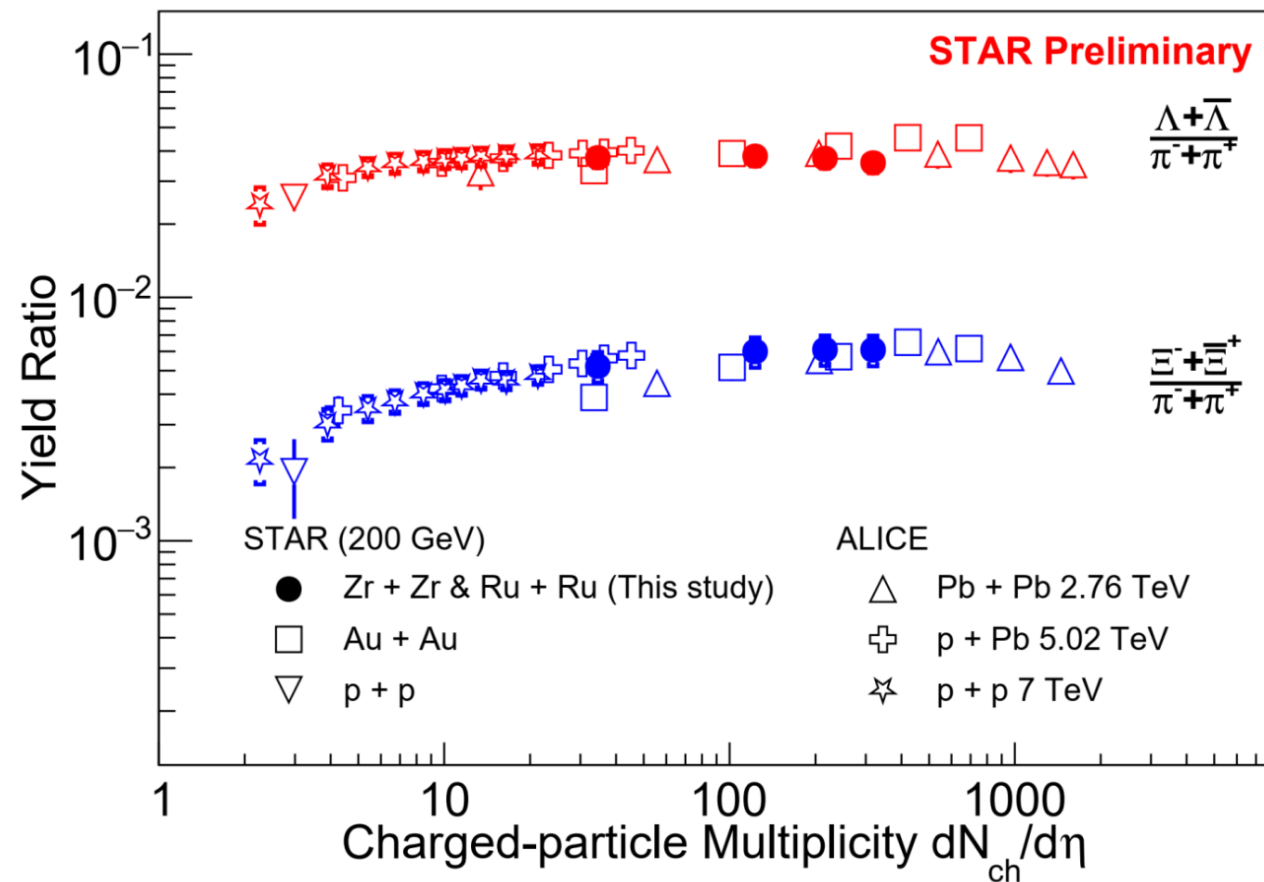
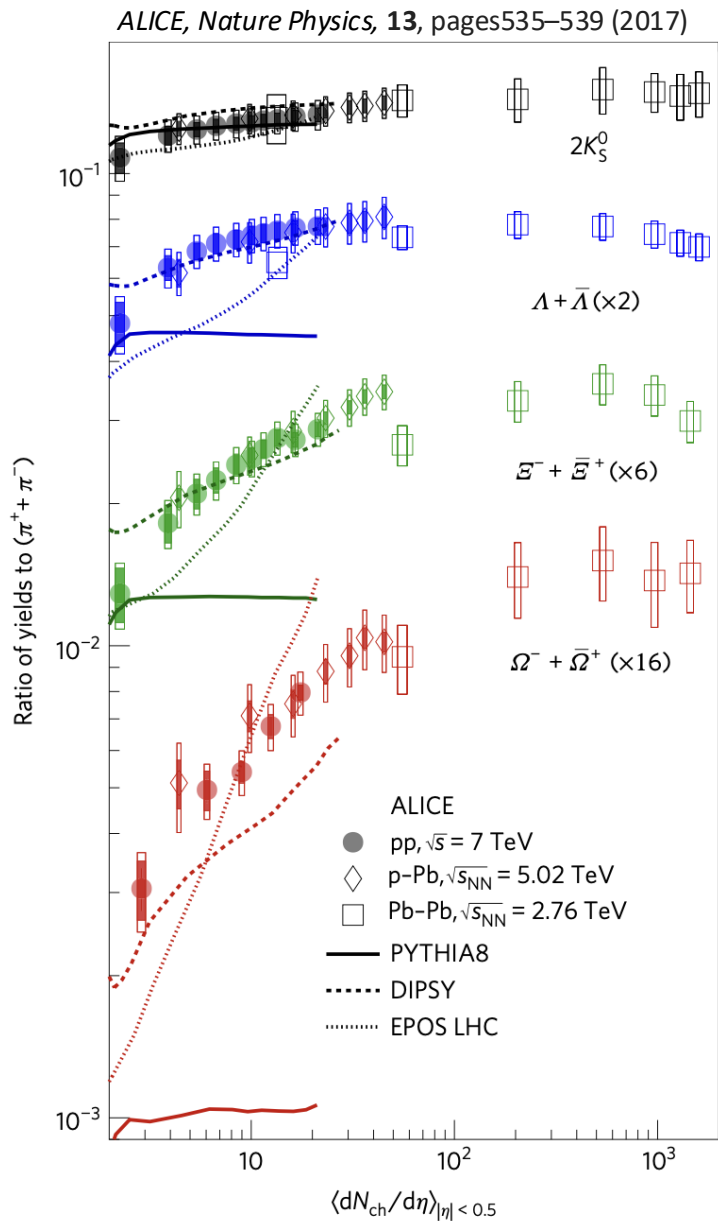
p+p: STAR, Phys. Rev. C 75 (2007) 064901

pub. Au+Au: STAR, Phys. Rev. Lett. 98 (2007) 062301

Cu+Cu: STAR, Phys. Rev. Lett. 108 (2012) 072301

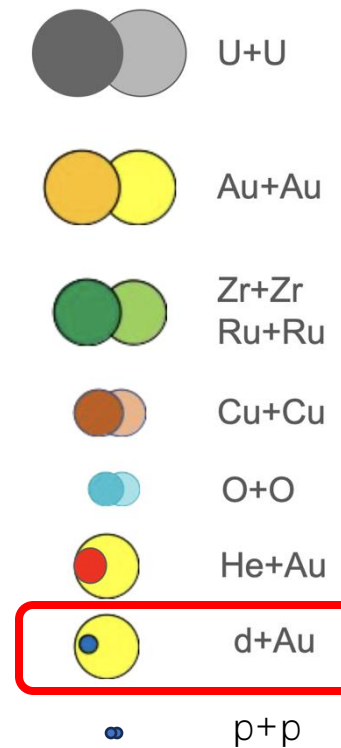
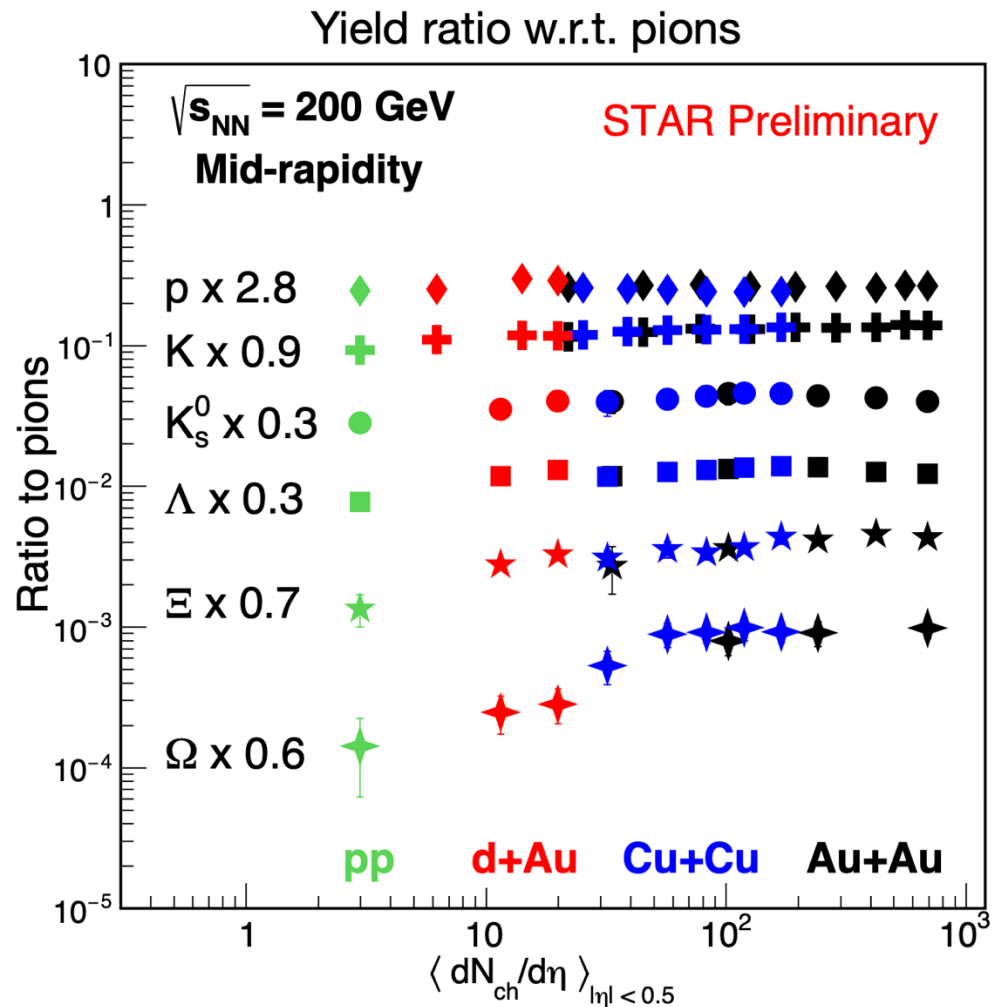
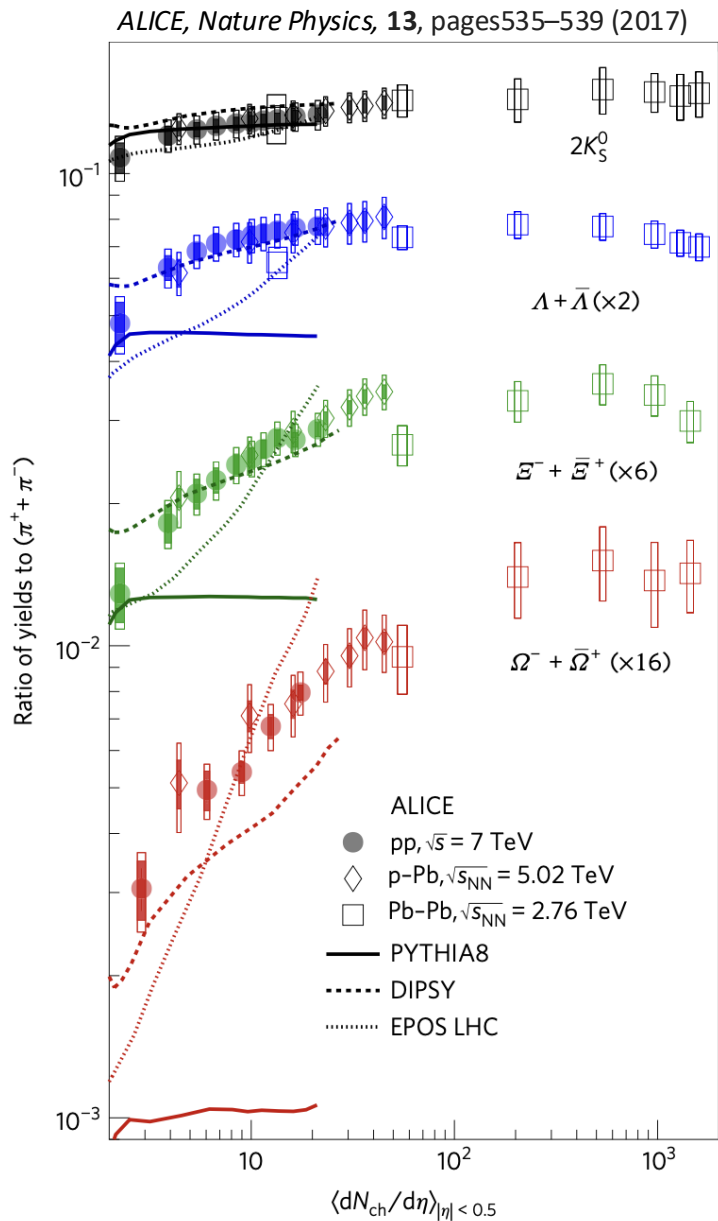
Other preliminary data, X. Zhu, QM2014

System size dependence of strange-to-pion yield ratios



- Isobar hyperon-to-pion ratios follow the trend.
- Similar hyperon production mechanism for systems with same multiplicity despite differences in collision energy or system.

System size dependence of strange-to-pion yield ratios

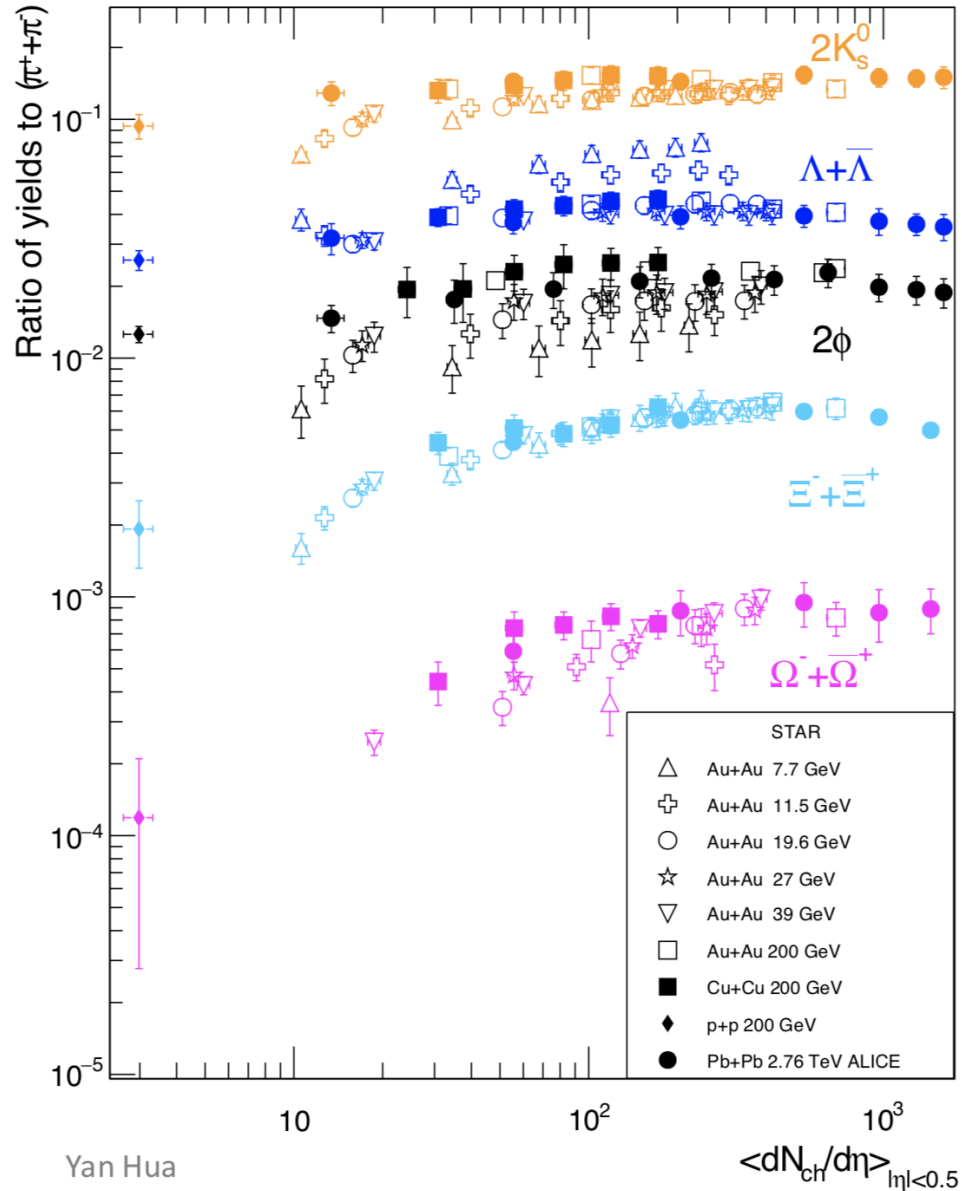


- Smooth transition from p+p to A+A.
- O+O and p+p analysis on-going.

Summary and outlook

- Comprehensive strangeness measurements in STAR BES and top energy collisions.
- Baryon enhancement is observed from 7.7 to 200 GeV → consistent with QGP formation.
- Strange hadron yields at central collisions cannot be described by GCE thermal model in FXT collisions, while hadron transport models work better.
- Multi-strange hadron production show strong system-size dependence, sensitive to multiple hadronic/partonic collisions.
- More strangeness measurements and model comparisons in STAR BES-II and top energies will help study the medium properties at almost-zero to high baryon densities, and at different system sizes.

Strange hadron to pion ratio vs $dN_{ch}/d\eta$



Yan Huang, APS April Meeting 2021, SQM2021

STAR, PRC96, 044904, 2017
 STAR, PRC102, 034909, 2020
 ALICE, PRC88, 044910, 2013

$$\frac{dn}{dy} = \frac{\sqrt{M(1 + \sinh^2 y)} dn}{\sqrt{1 + M \sinh^2 y} d\eta'}$$

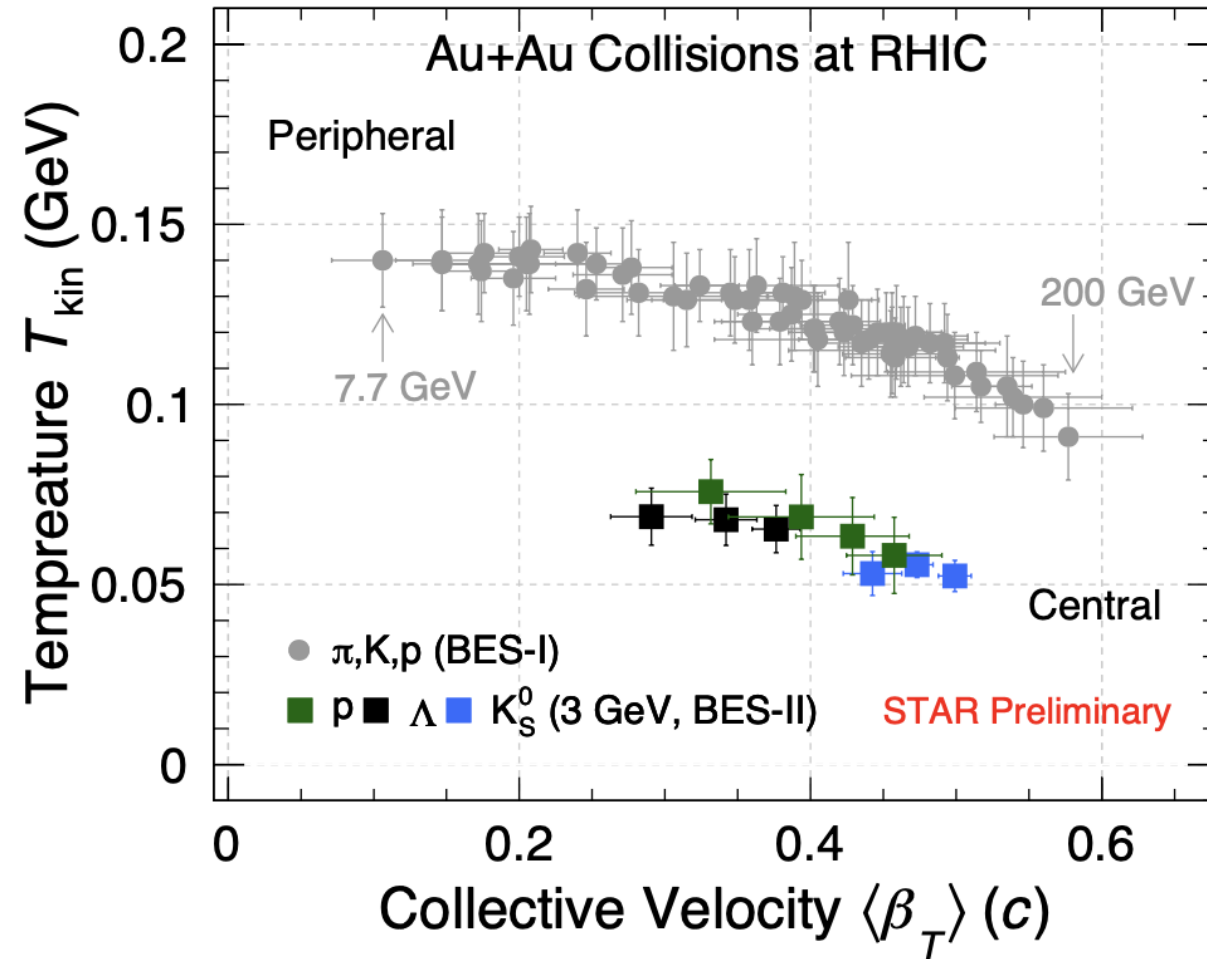
$$\text{where } M = 1 + m^2/p_t^2$$

$$dN_{ch}/d\eta = \sum dN_{ch}/d\eta (k^\pm, \pi^\pm, p, \bar{p})$$

$$dN_{ch}/d\eta(\eta = 0) \sim dN_{ch}/d\eta(|\eta| < 0.5)$$

- The ratios at different energies/centralities/systems mainly depend on charged hadrons multiplicity, except for Λ and ϕ
- The ratios saturate at large charged hadrons multiplicity

Kinetic freeze-out properties at 3 GeV

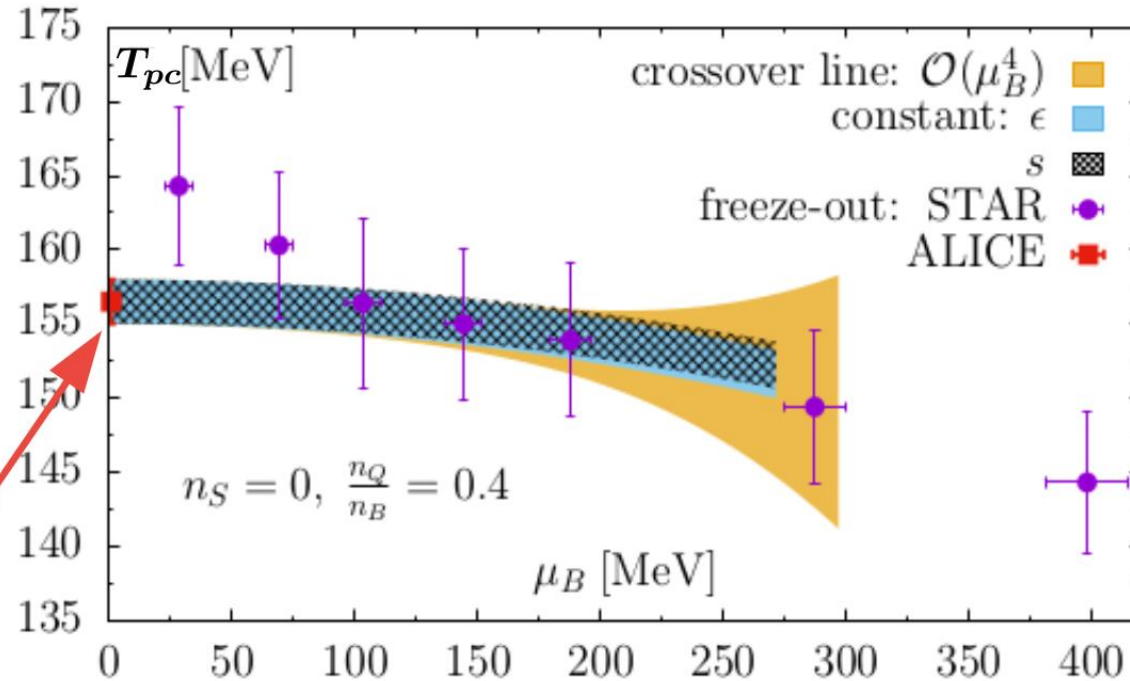


- T_{kin} of Λ and K_S^0 at 3 GeV is lower than π, K, p at higher energy collisions
- Similar observations for protons and deuterons, implying different EOS at freeze-out

Pseudo-critical line for physical quark mass values

$$T_{pc}(\mu_B) = T_{pc}(0) \left(1 - \kappa_2 \left(\frac{\mu_B}{T_{pc}(\mu_B)} \right)^2 - \kappa_4 \left(\frac{\mu_B}{T_{pc}(\mu_B)} \right)^4 + \dots \right)$$

phase diagram at
physical values of
the quark masses



STAR:
arXiv:1701.07065
A. Andronic et al.,
Nature 561 (2018)
321

$$T_{pc} = (156.5 \pm 1.5) \text{ MeV}$$

$$\kappa_2 = 0.012(4)$$

$$\kappa_4 = 0.000(4)$$

A. Bazavov et al. [HotQCD],
Phys. Lett. B795 (2019),
arXiv:1812.08235

$$T_{pc} = (158.0 \pm 0.6) \text{ MeV}$$

$$\kappa_2 = 0.0153(18)$$

$$\kappa_4 = 0.00032(67)$$

S. Borsanyi, et al,
PRL 125 (2020)
arXiv:2002.02821

F. Karsch, iHIC24

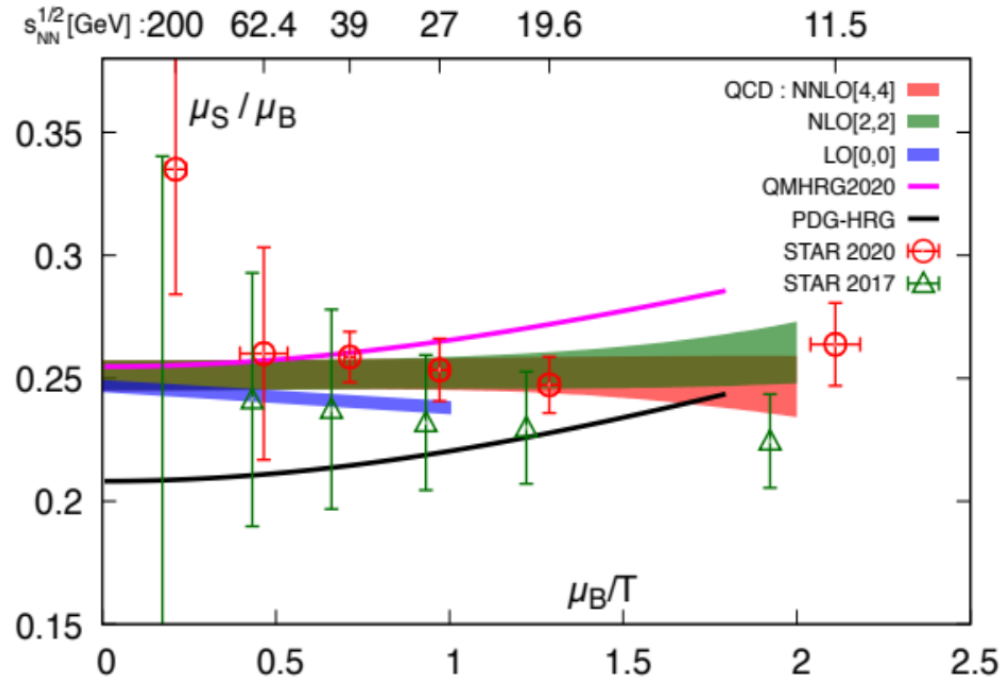
Baryon number – strangeness chemical potentials at freeze-out from strange baryon yields vs. QCD

QCD:

$$\frac{\mu_S}{\mu_B} \equiv -\frac{\chi_{11}^{BS}}{\chi_2^S} - q_1 \frac{\chi_{11}^{QS}}{\chi_2^S} + \mathcal{O}(\mu_B^2)$$

STAR:

$$\ln(\bar{B}/B) = -2\mu_B/T_{ch} + \mu_S/T_{ch} \cdot \Delta S$$



F. Karsch, iHIC24

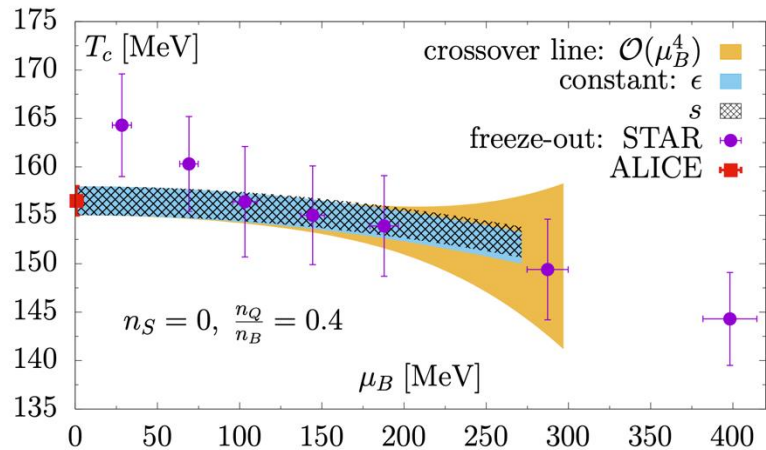
HotQCD, Phys. Rev. D 104 (2021) 074512
arXiv:2107.10011

STAR2017: Phys. Rev. C 96 (2017) 044904
STAR2020: Phys. Rev. C 102 (2020) 034909

STAR multi-strange baryon yields are consistent with freeze-out at T_{pc} and a μ_S/μ_B that reflects contributions from additional strange baryons

Extracting chemical freeze-out parameters in BES-II

HotQCD, PLB 795 (2019)



- Uncertainties dominated by systematics in yields of charged hadrons (5% tracking uncertainty in TPC)
- Pinning down these uncertainties in BES-II with iTPC and improved detector simulation.

